Preprints.org

Article

Covalent Conjugates of Allylbenzenes and Terpenoids as Antibiotics Enhancers with the Function of Prolonged Action

Igor D. Zlotnikov , Maria P. Davydova , Milan R. Danilov , Sergey S. Krylov , Natalia G. Belogurova ,

Elena Vadimovna Kudryashova *

Article

Covalent Conjugates of Allylbenzenes and Terpenoids as Antibiotics Enhancers with the Function of Prolonged Action

Igor D. Zlotnikov [1,*], Maria P. Davydova [2], Milan R. Danilov [1], Sergey S. Krylov [3], Natalya G. Belogurova [1] and Elena V. Kudryashova [1,*]

[1] Faculty of Chemistry, Lomonosov Moscow State University, Leninskie Gory, 1/3, 119991 Moscow, Russia; nbelog@mail.ru (N.G.B.)

[2] Faculty of Medicine, Lomonosov Moscow State University, 27/1, Lomonosovsky prosp., 119192 Moscow, Russia; dawydova2015@gmail.com

[3] N. D. Zelinsky Institute of Organic Chemistry RAS, 47 Leninsky Prospect, 119991 Moscow, Russia

* Correspondence: zlotnikovid@my.msu.ru (I.D.Z.); helena_koudriachova@hotmail.com (E.V.K.)

Abstract: The drug resistance of pathogenic bacteria is often due the work of efflux pumps - specific proteins that remove foreign compounds from bacterial cells. To overcome drug resistance, adjuvants are often used that can inhibit efflux pumps or other systems that ensure the resistance of bacteria to the action of antibiotics. We assumed that a new level of effectiveness with the use of an antibiotic + adjuvant pair could be achieved by their joint delivery into the pathogen. To test this hypothesis, we have constructed a series of molecular carriers based on the mannosylated poly-(olygo-, dendry)mers based on cyclodextrin-grafted PEI or mannan, as well as glycol-chitosan, covalently bound to a model antibiotic, adjuvant, and mannose receptor oligosaccharide ligand to macrophage (CD206), which we studied earlier and showed high efficiency and selectivity of delivery of therapeutic "cargo" to macrophages. Moxifloxacin was used as a model antibiotic, and terpenoid and allylbenzene compounds were used as adjuvants, for which we previously discovered the ability to inhibit bacterial efflux pumps. We have shown that: a) the resulting structures are stable in vitro for a long time (up to 5 days); b) they are adsorbed on bacterial cells, providing a local increase in the concentration of the antibiotic and adjuvant in pathogen cells; c) they are internalized by bacterial cells, ensuring the accumulation of both antibiotic and adjuvant inside bacterial cells; d) adjuvant, after getting inside the bacterial cell, provides inhibition of efflux pumps; e) due to this action of the adjuvant, combined with targeted delivery by the carrier, the antibiotic's half-life in rat increases by more than 2 times; f) a significant increase in the effectiveness of antibacterial action against gram+ and gram- cells has been achieved (up to 2-3 times). Potentially, such an approach would significantly increase the effectiveness of therapy for a number of infectious and other diseases, reduce the dosage of antibiotics, shorten the duration of treatment, and reduce the risk of developing resistance. Moreover, the use of a polymer carrier with covalently bound organic molecules of different structures avoids problems with different (suboptimal) solubility and bio-distribution, which would be almost inevitable when using the same compounds separately. It would be very difficult to find antibiotic/adjuvant pairs that simultaneously achieve optimal concentrations in the same target cells. In our case, terpenoids and alkylbenzenes used as adjuvants are practically insoluble as individual compounds and their unacceptable pharmacological properties would not allow them to be used as efflux pump inhibitors.

Keywords: covalent antibacterial conjugate; moxifloxacin; limonene; prolonged pharmacokinetic; FTIR spectroscopy

1. Introduction

Infections caused by pathogenic bacteria are one of the main causes of death in developing countries and a serious health problem in developed countries. The widespread use of antibiotics leads to the emergence and development of resistant and multi-resistant strains resistant to several types of antibiotics at the same time, as well as reservoirs of latent or "dormant" bacteria. Multidrug resistance (MDR) is a growing global problem: every year about 2.5 million people worldwide die

from resistant bacterial infections. By 2050, it may grow to 10 million people a year. Among the main mechanisms of the emergence of resistance are the poor penetration of antibiotics into the localities of latent infection, as well as the work of efflux pumps - specific proteins that remove drug compounds from bacterial cells [1].

Targeted delivery to macrophages opens up numerous opportunities to influence a wide range of diseases and pathological conditions, of which they are the driver or participant [2–9,9–27]. The developed highly effective systems for delivering antibacterial drugs to macrophages are able to increase the effectiveness of therapy by directly affecting the reservoir of latent infection localized in them. Systematic studies of CD206 ligands conducted by our group [6,19,28–32] allowed us to develop a specific molecular container carrying an oligomannoside ligand of complex structure with optimal affinity to mannose receptors of macrophages. We modeled the interaction of CD206 with more than a hundred relevant carbohydrate structures, of which about two dozen were studied experimentally. As a result, optimized polymer ligands provide the effect of accumulation of therapeutic "cargo" in macrophages, which significantly increases organ bioavailability (bio-distribution and accumulation of drugs in the lungs), increases the permeability of drugs into bacterial cells.

Additionally, a significant increase in efficiency can be achieved by using adjuvants that increase the permeability of bacterial cells to the antibiotic and inhibit efflux proteins of bacteria ("throwing" the drug out of the cells), which can significantly increase the accumulation of the main drug in bacterial cells. As adjuvants in our scientific group, compounds of the terpenoid and flavonoid series are extensively studied, which show synergism with the main drug - antibiotics MF, levofloxacin, rifampicin, etc. Terpenoids and flavonoids are extracts from essential oils of plants that exhibit a number of remarkable biological effects [6,28,33–41], including analgesic, antibacterial, anti–inflammatory, and antioxidant activity.

However, they are insoluble in aqueous media - limiting their positive effects for practical application. The molecular containers we are developing, allow us to realize their potential and achieve their synergistic effect with antibiotics: when the combined preparation of fluoroquinolone and its adjuvant are included in the delivery system, a dual mechanism of action of adjuvants is shown: increasing the permeability of bacterial cells to the antibiotic and inhibiting the efflux of bacterial proteins, which allows to increase the accumulation of drugs in bacterial cells. So, for the combination of fluoroquinolone – terpenoid, we observed a 2-3-fold increase in the effectiveness of the antibiotic (a 2-3-fold decrease in MIC) [42–44].

However, the binding constants of MF and adjuvants with the developed molecular containers - polymer ligands are not strong enough (about 10^{-4} M), which assume premature dissociation of complexes upon intravenous administration and does not provide for prolonged action of the antibiotic.

In the presented article, we aimed to create a moxifloxacin prodrug – a covalent conjugate of the antibiotic with mannosylated polymers (dendrimers) based on cyclodectrin-grafted PEI or mannan enhanced by a terpenoid adjuvant with the function of prolonged action, in which long-term circulation in the bloodstream is expected. As a comparison system, of the same antibacterial agents included in polymeric nanogels crosslinked using biodegradable bifunctional agents, such as genipin [45–50] and acetylcysteine derivatives, which provide the formation of disulfide bonds between polymer chains, are considered. Potentially, the approach suggested would significantly increase the effectiveness of therapy for a number of infectious and other diseases, reduce the dosage of antibiotics, shorten the duration of treatment, and reduce the risk of developing resistance. Moreover, the use of a polymer carrier with covalently bound organic molecules of different structures avoids problems with different (suboptimal) solubility and bio-distribution, which would be almost inevitable when using the same compounds separately. Creation of such formulation is expected to be perspective in terms of increased in the effectiveness and safety of therapy for infectious diseases such as tuberculosis, pneumonia, pulmonary fibrosis, gastrointestinal inflammation.

2. Results and Discussion

2.1. Synthesis and characterization of covalent and non-covalent antibacterial formulations

To to reveal the role of prodrug creations by the covalent attachment of antibacterial agents (moxifloxacine (MF) enhansed by terpenoids or allylbenzenes adjuvant) to mannosylated polymers based on cyclodectrin-grafted PEI or mannan, as well as glycol-chitosan are considered. The mannose label is important for targeted delivery of a polymer with an antibacterial drug to the sites of localization of pathogens – to macrophages. We expect that covalent conjugates could show prolong antibacterial action as well as enhanced antibacterial activity due to their higher local concentration in the vicinity of the areas of inflammation, additionally, they could circulate in the blood flow much longer compared to non-covalent antibacterial formulations. An important task is to compare prodrug where MF is conjugated through an amide bond and through a ethereal bond: firstly, from the point of view of optimal synthesis tactics, secondly, antibacterial activity of this prograds (conjugates), and thirdly, prolonged action of the drug as well as the synergistic effect of antibiotics with adjuvants.

As an alternative option for creating a composition (MF+adjuvant) with the function of prolonged action and increased efficiency, we proposed th aapproach based on the inclusion of the drug in the gel, followed by crosslinking with biodegradable and stimulus-sensitive bifunctional crosslinking agents (with spontaneously and reversibly formed disulfide bonds or through the formation of imide bonds of amino groups of polyimines (PEI, chitosane) with genipin). In this case the MF-formulation is realised without the involvement of functional groups of antibiotics in th covalent coupling.

To realize these strategy, we focused on the following points:

1) Synthesis and characterization by FTIR and NMR spectroscopy of covalent conjugates of MF, allylbenzenes (EG and apiol), terpenoids (linalool and limonene) with polymers (based on PEI, chitosane, mannan) with a variable type of covalent linkage (amide or ester bond) and with a variable crosslinking agent to determine the most efficient and optimal composition of the antibacterial conjugate.

2) Incorporation of the drug composition into polymer nanogels followed by covalent crosslinking of particles, but without involving the drug in covalent bonds.

3) The antibacterial activity stidy (against E. coli and B. subtilis) of prodrags developed in terms of efficiensy and duration of their action.

4) Elucidation of the mechanisms of conjugate action on cells using FTIR spectroscopy in comparoson with free antibacterials.

5) Study of pharmacokinetics of antibacterial covalent prodrugs in comparison with antibacterial formulation included in nanogels (non-covalent prodrugs).

2.1.1. MF covalent prodrug formulations synthesis and characterization by FTIR and NMR spectroscopy

Figure 1a-c shows the FTIR spectra and structures of conjugates MF-polymer. The crosslinking of MF and polymers is realized due to amide (in the case of HPCD-PEI1.8-triMan and GlycChit) or ester (in the case of mannan) bonds (Figure A1 – appendix), which have characteristic peaks in the FTIR spectra: 1710, 1650 and 1700-1740 cm^{-1}, corresponding to valence oscillations of C=O (in the specified order, amide bond – peak at 1650 cm^{-1} (Figure 1a,b) and the ester bond is visible by splitting the peak at 1710-1740 cm^{-1} (Figure 1c)). FTIR spectra of conjugate contain peaks, characteristic of both MF (ν(C=C) 1400-1600 cm^{-1}, ν(C–H) 2850-2970 cm^{-1}) and polymers (C-O-C 1000-1100 cm^{-1}). It is assumed that, the ester bond is easier to hydrolyze than the amide bond, which is more stable and is hydrolyzed enzymatically by plasma proteases, which will potentially affect the properties of conjugates in terms of antibacterial activity and pharmacokinetic parameters.

The successful synthesis is confirmed by NMR spectroscopy data (Figure 1d,e): both polymer signals (2.5-4.0 and 5.0-5.5 ppm) and characteristic signals for aromatic MF protons (7.2-9.0 ppm) are present in the composition. With covalent crosslinking of MF, MF signals shift into a weak field.
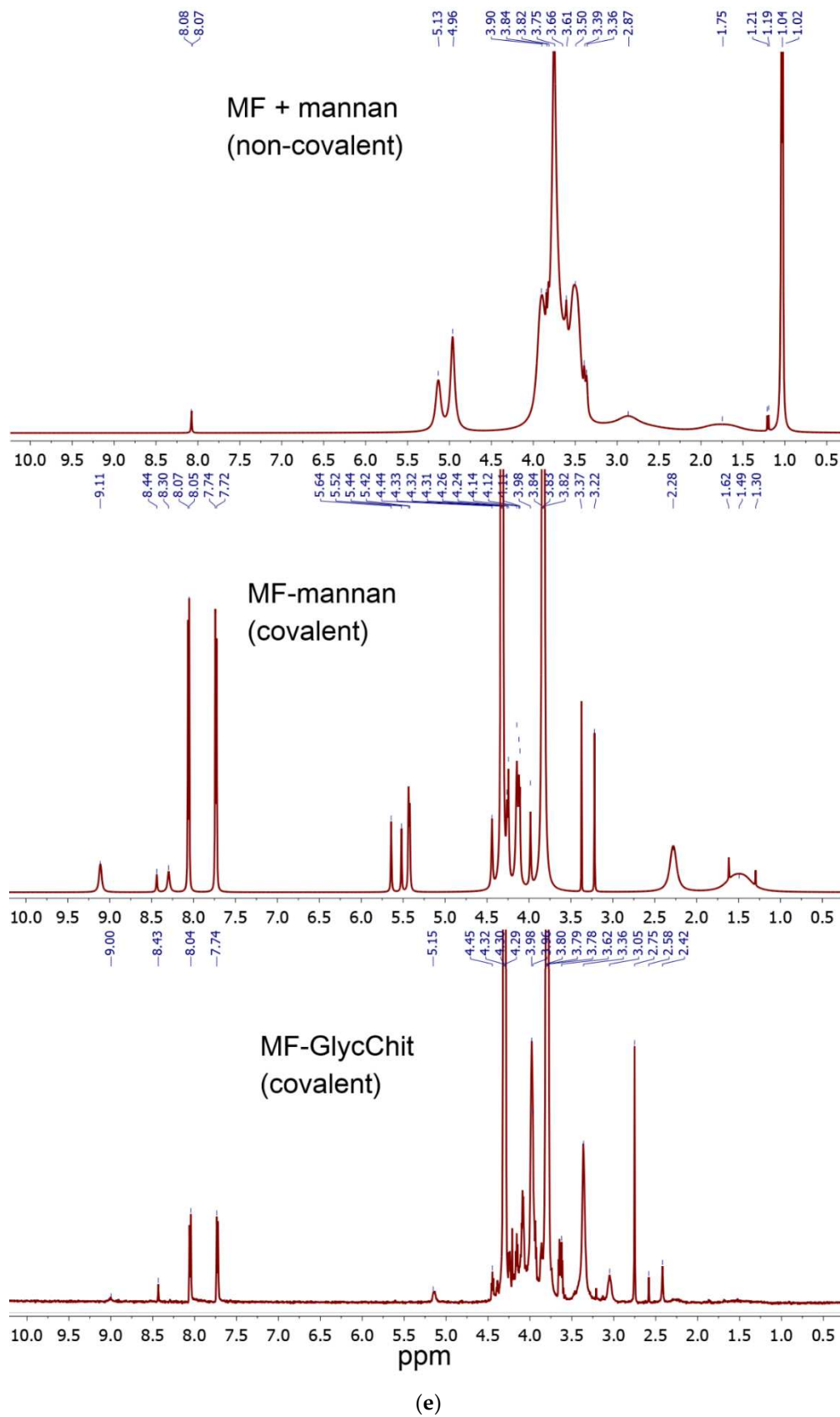
4

(**a**)

(**b**)

(c)
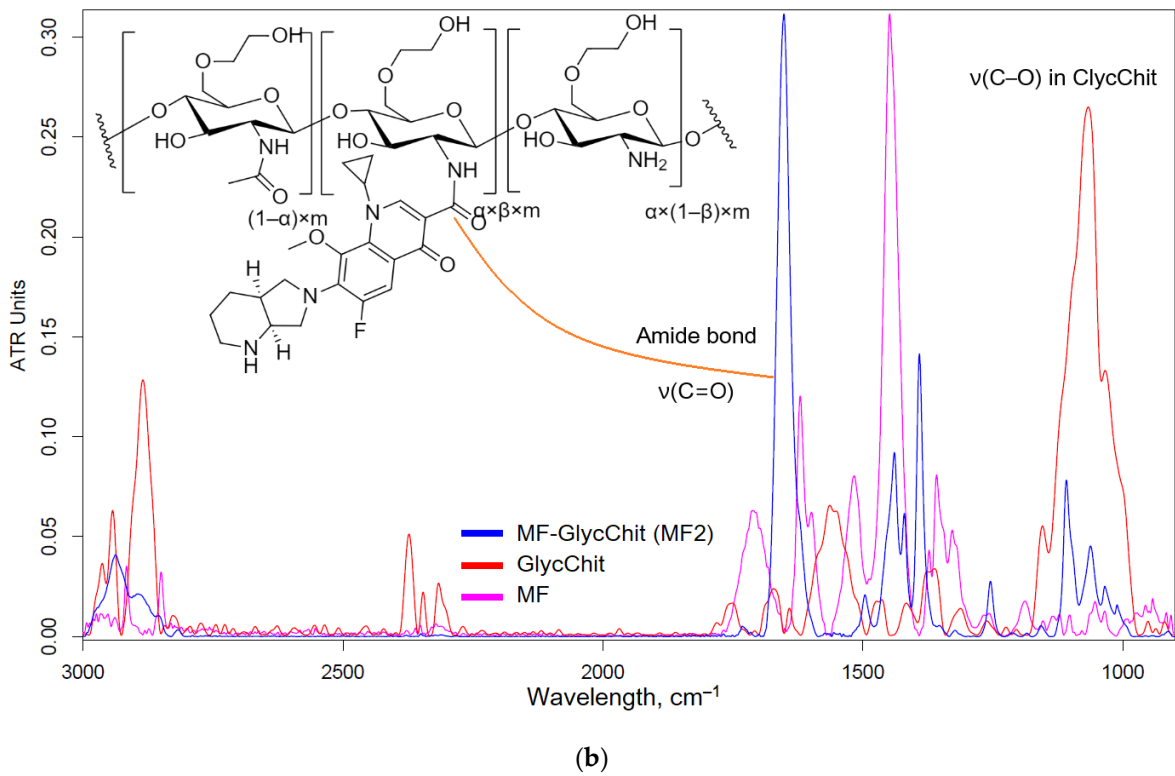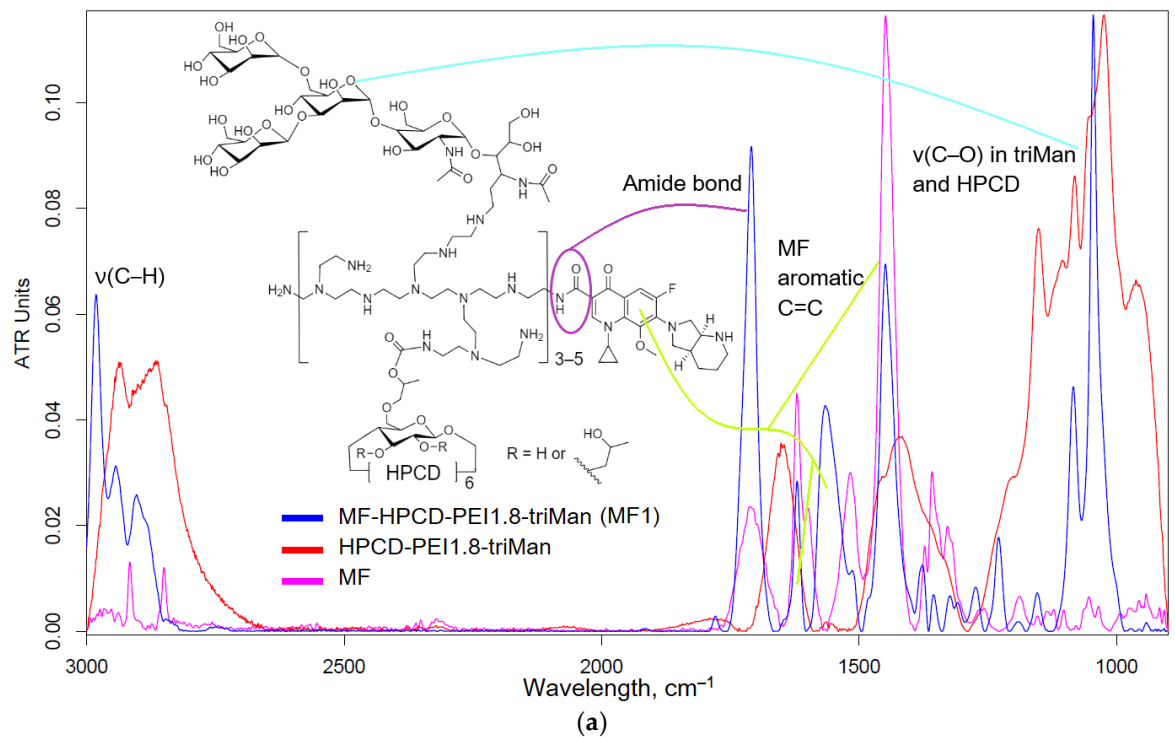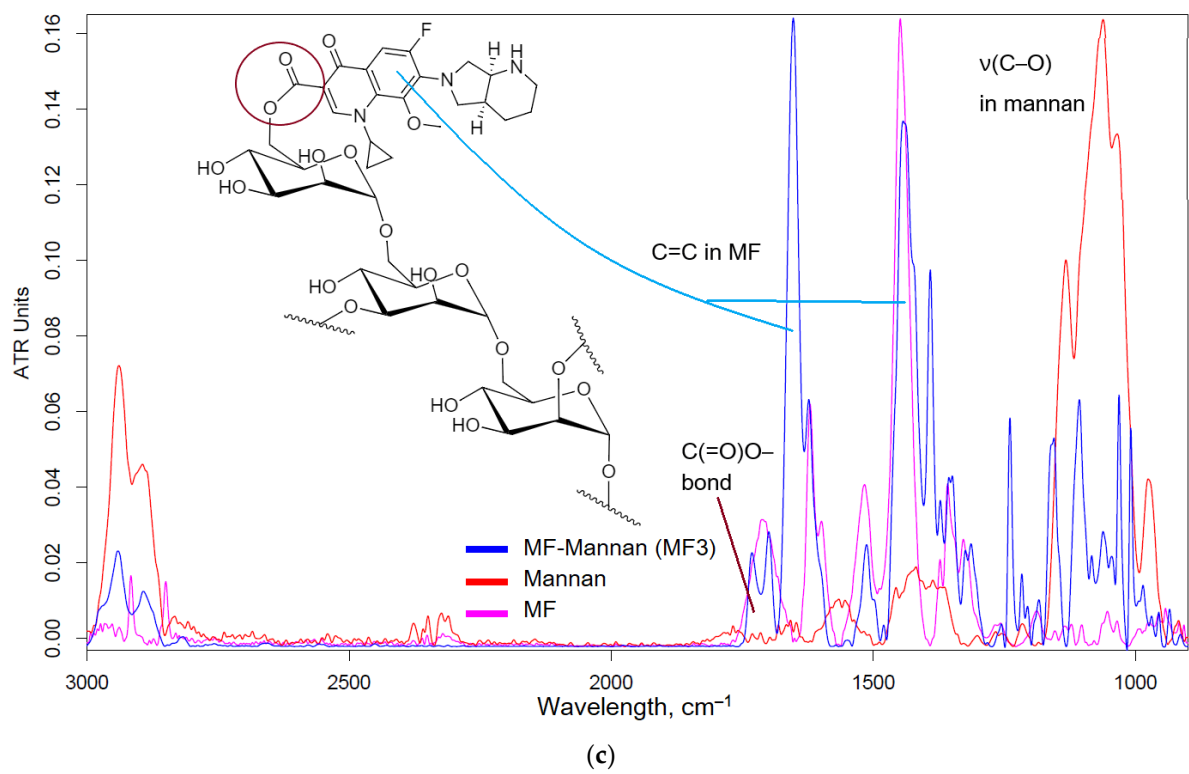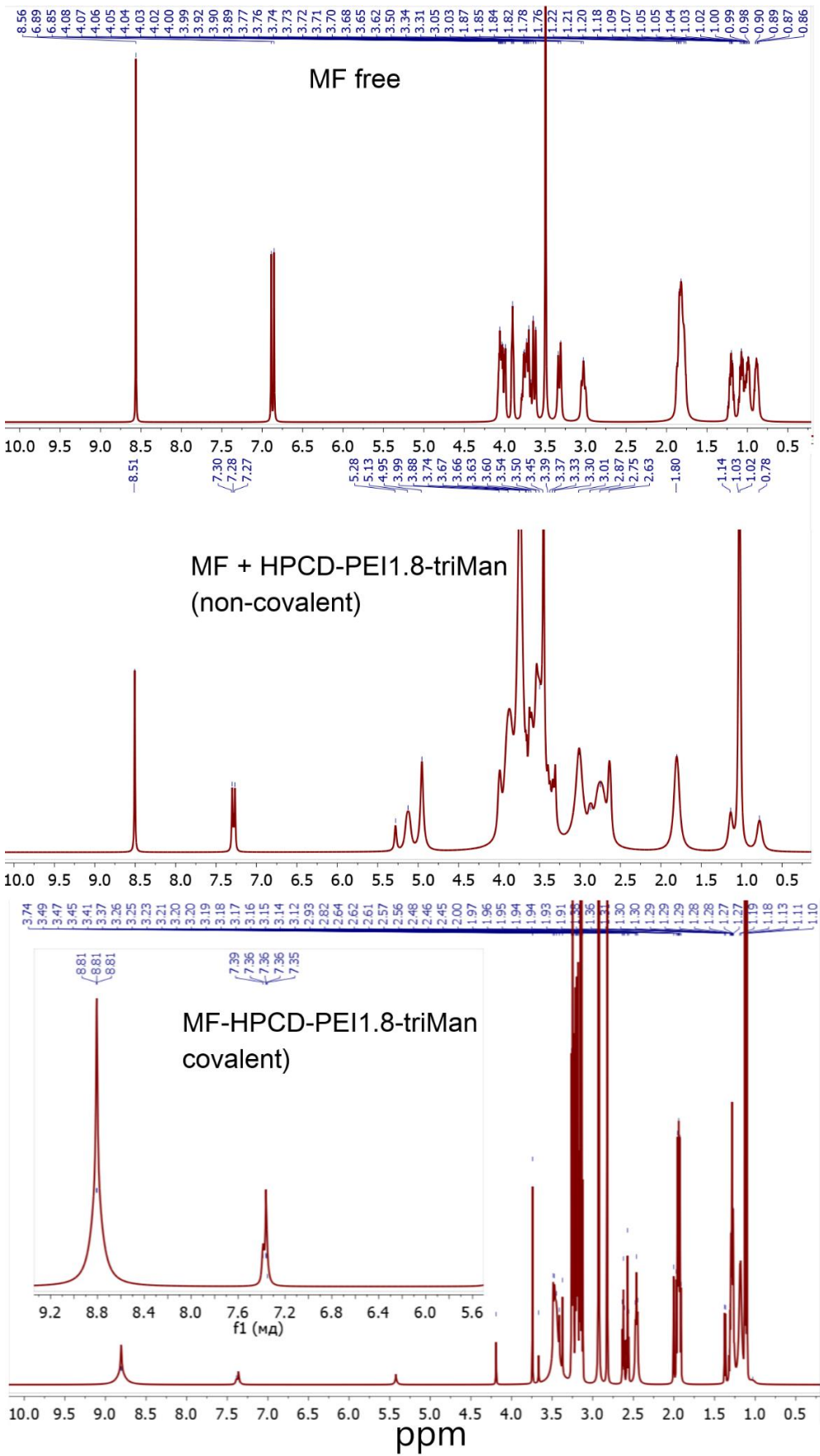
(d)

Figure 1. FTIR spectra of MF, polymers and conjugates MF-polymer based on: (a) HPCD-PEI1.8-triMan, (b) GlycChit, (c) Mannan. PBS (0.01M, pH 7.4). T = 22 °C. ^{1}H NMR spectra of MF, mixtures and conjugates MF-polymer based on: (d) HPCD-PEI1.8-triMan, (b) GlycChit and Mannan. D$_2$O. T = 25 °C.
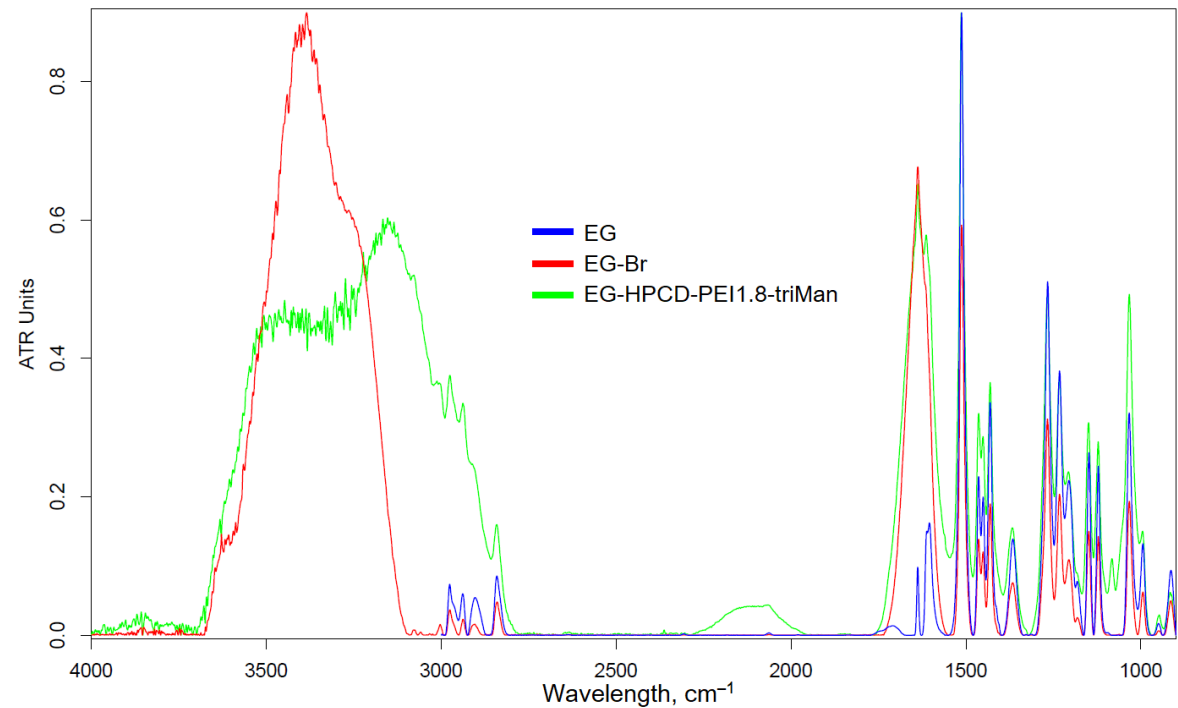
2.1.2. Allylbenzenes and terpenoids formulations

The components of plant oils (eugenol (EG) and terpenoids) demonstrate antibacterial activity, weaker in comparison with classical antibiotics, but sufficient to partially replace them, i.e. reduce the dosage of toxic drugs and have an enhancing effect on the main component (in this work – MF). One of the tasks of the work is to obtain soluble forms of allylbenzenes and terpenoids due to their conjugation with polymers or inclusion in polymer particles.

Figure 2a shows a scheme for the synthesis of covalent conjugates of EG, apiol, linalool and limonene with HPCD-PEI1.8-triMan. The first stage is the addition of HBr to C=C, accompanied by a change in shape (broadening) and an increase in FTIR peak intensity by 1600-1800 cm^{-1} (Figure 2b-e), characteristic of ν(C=C) oscillations in aromatic system or double bond. The second stage is the nucleophilic substitution of a bromine atom in allylbenzene or terpenoid molecule by amino-group of HPCD–PEI1.8-triMan polymer, accompanied by the appearance or change of a peak by 3000-3600 cm^{-1} (valence oscillations of O–H, N–H) due to contribution of polymer functional group. An increase in peak (C-O-C 1000-1100 cm^{-1}) intensity also indicates the presence of a polymer in the final product.

Thus, FTIR spectroscopy confirms the formation of covalent conjugates of allylbenzenes, terpenoids, MF with polymers. However, covalent attachment can lead to loss or decrease in biological activity, so for comparison (as control system) we also synthesized covalently crosslinked nanogels where antibiotics and its adjuvant included in the formulations non-covalently as discussed above.

(**a**)

(b)

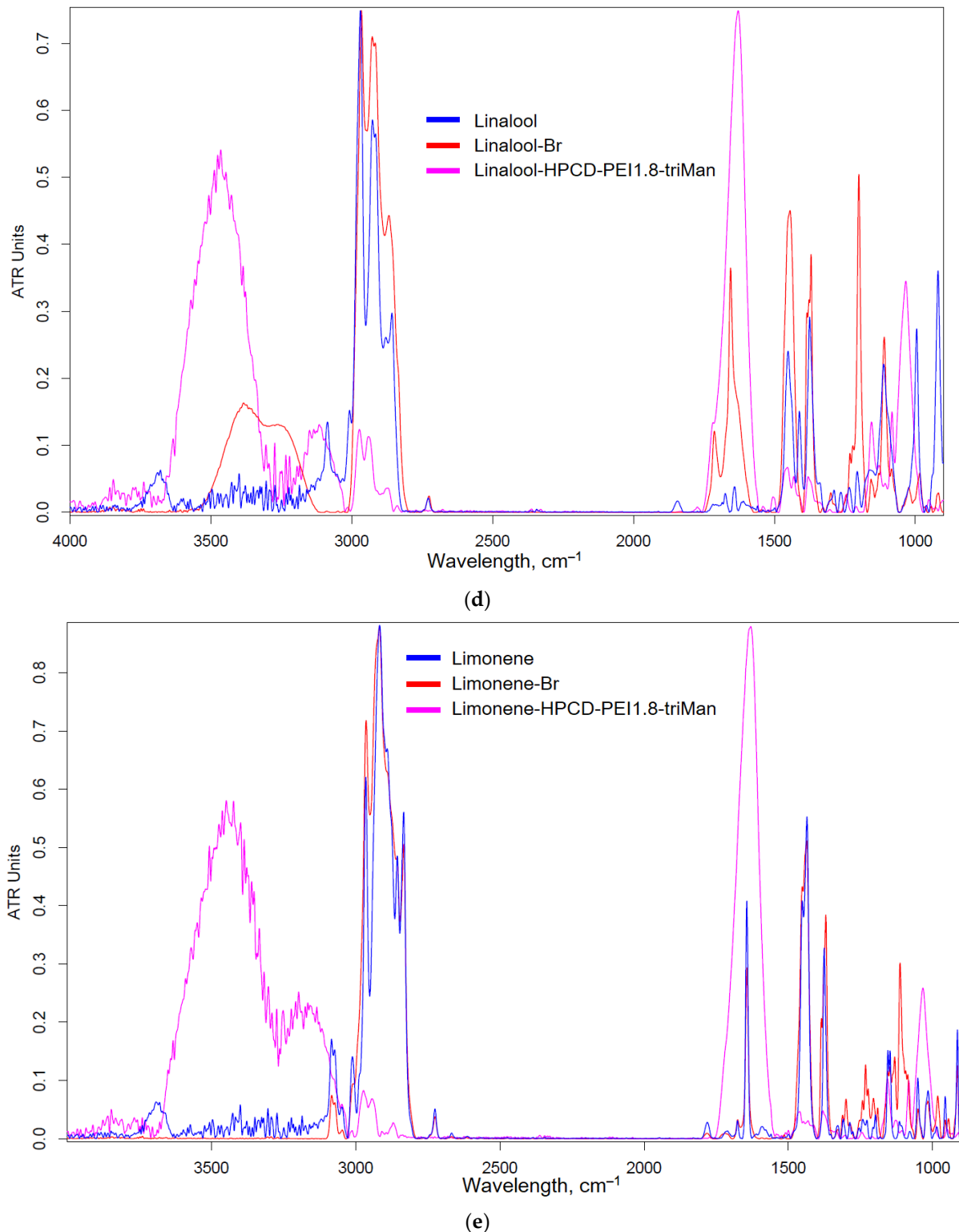**(c)**

(d)

(e)
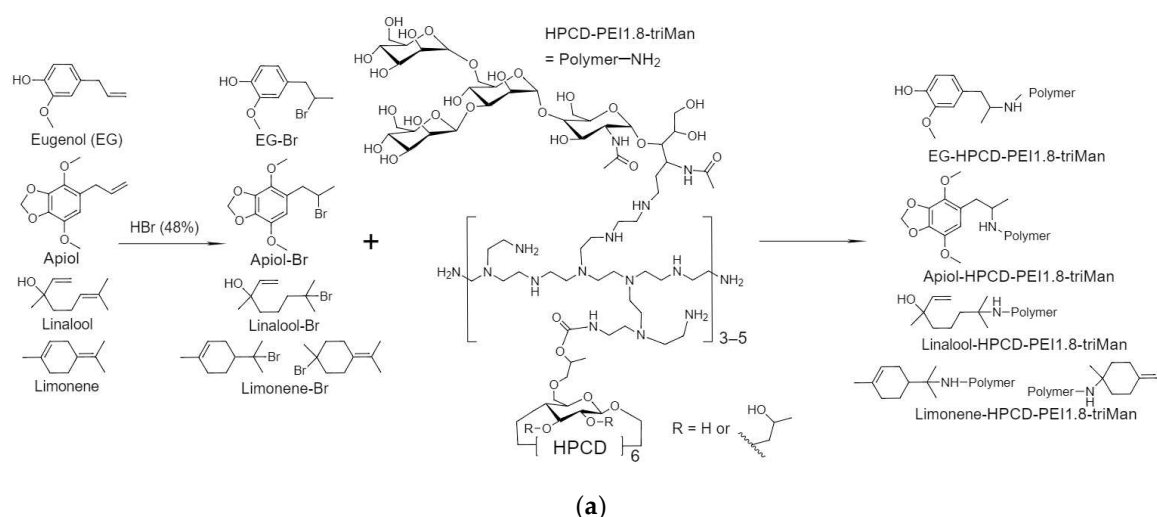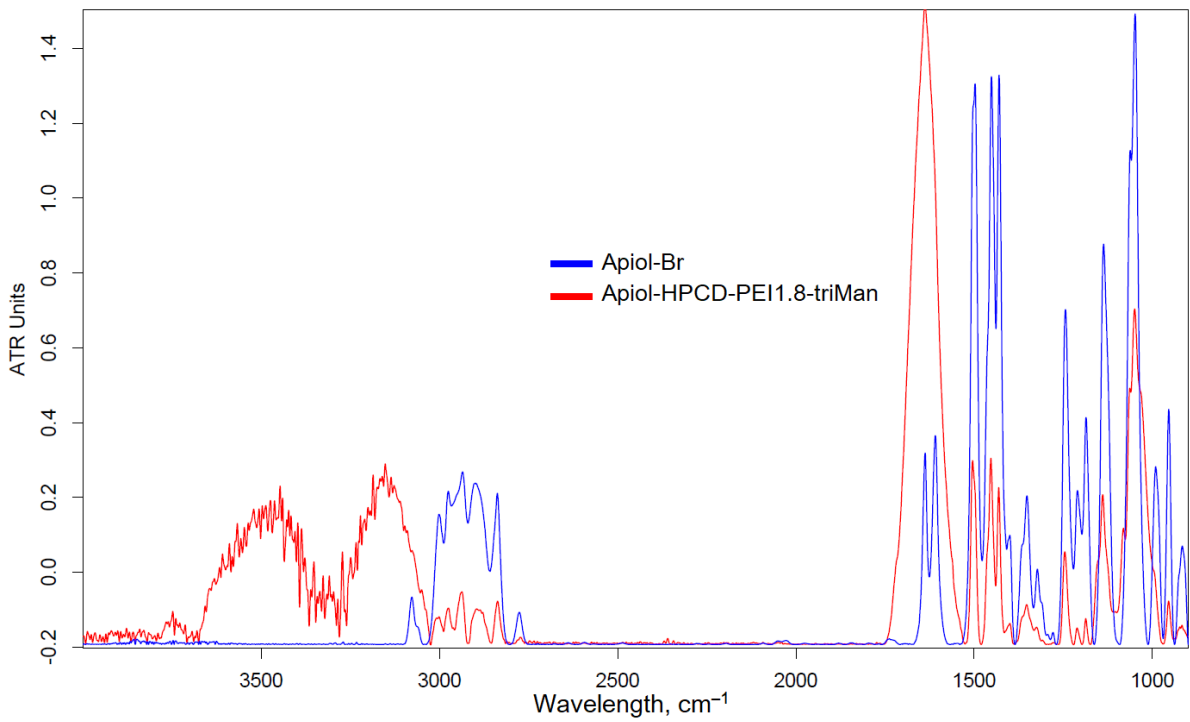
Figure 2. (a) Synthesis scheme and FTIR spectra of (b) EG, (c) apiol, (d) linalool, (e) limonene, their bromine derivatives and conjugates with polymers. T = 22 °C.

2.1.3. Non-covalent formulations of MF, allylbenzenes and terpenoids with glycol-chitosan hydrogels stabilized by crosslinking bifunctional agents

Non-covalent formulations of combined antibacterials were obtained by including of antibacterial agents into polymer particles followed by the crosslinking polymer chains with each other. For such systems it is expected that biological (anti-inflammatory, antioxidant, antibacterial, antitumor) properties are not lost or even increased. A number of crosslinking agents have been

described in the literature: glutaraldehyde [51,52], diisocyanates [53], but having toxic properties. In this work, biocompatible and even medically "useful" crosslinking agents were used: genipin [54–61] and N-acetylcysteine. Genipin (from clove oil) is able to crosslink chitosan amino groups in different chitosan polymer chains due to the formation of an amide and amine bonds (Figure 3). As a second variant, we propose a new pH- and stimulus-sensitive acetylcysteine cross-linked (attached to chitosan by carbodiimide method) chitosan with the formation of S-S bonds (nanogel forms spontaneously when chitosan polymeric chains fold and this reaction is reversible and can be regulated by the conditions changes).
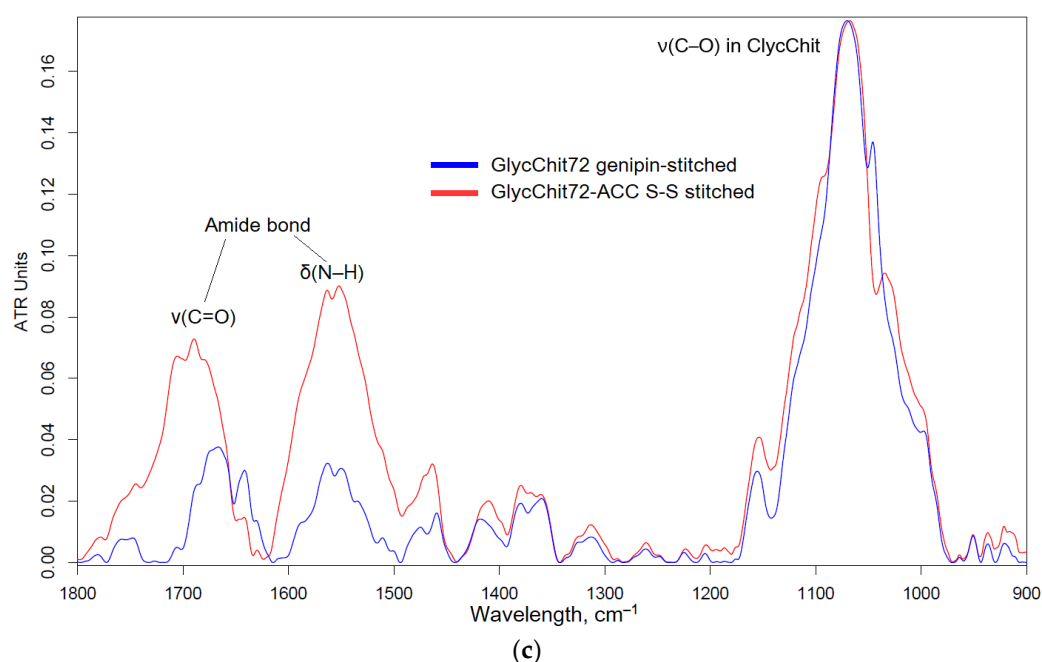

(a)

(b)

(c)
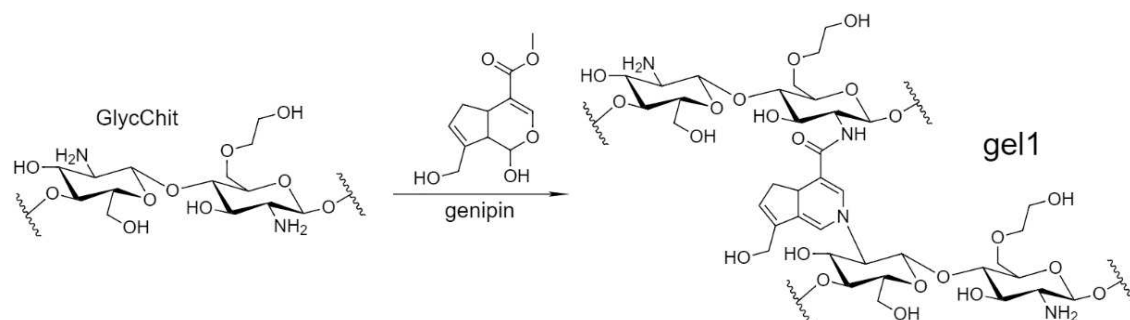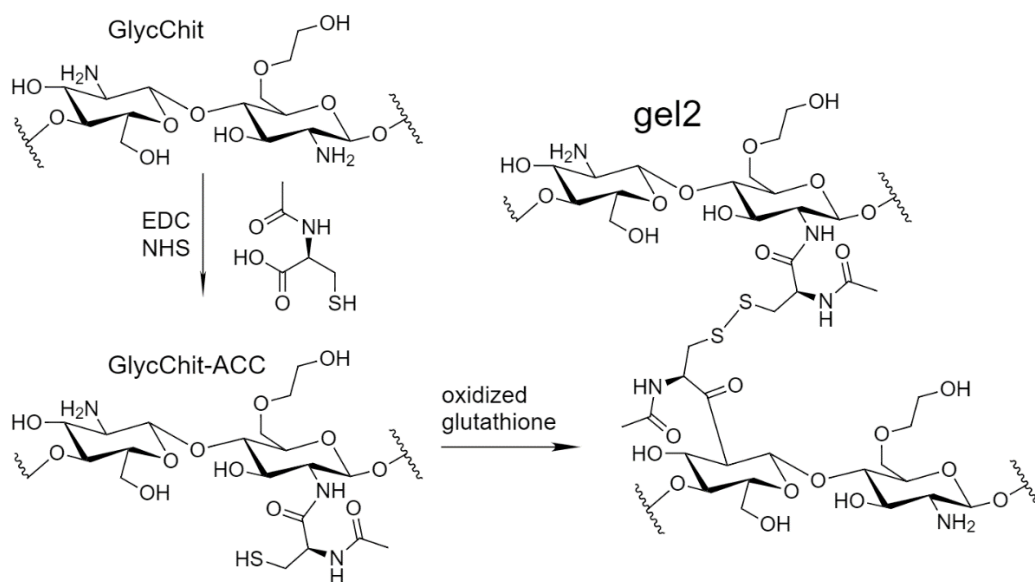
Figure 3. The scheme of synthesis of (a) genipin-stitched GlycChit, (b) N-acetylcysteine stitched GlycChit, and their FTIR spectra (c).

2.2. Antibacterial activity of MF, allylbenzenes, terpenoids

2.2.1. Primary high throughput screening of antibacterial activity of prodrug – conjugates

To find the most efficient antibacterial agent or a combination of them, we conducted a primary screening of the activity of MF as well as allylbenzenes and terpenoids conjugates in covalent prodrug and in the formulation of non-covalent nanogel for the samples demonstrated pronounced antibacterial activity.

Figure 4 shows the curves of cell growth dependence on incubation time with antibacterials formulations - as a primary screening analysis of the effectiveness of MF and adjuvants. Tables 1 and 2 show quantitative characteristics of the antibacterial activity of covalent prodrugs (in conjugates) and in nanogel. In the case of MF, in the result of the covalent attachment to the polymer, the value of half maximal inhibitory concentration (IC50) against *E. coli* decreases due to increased adsorption of MF resulting to higher drug efficacy [62]. This effect is clearly observed against gram-positive *B. subtilis*, where free MF (non-formulated) acts much worse, while the conjugate acts pronounced brighter.

The effectiveness of the drug is also characterized by kinetic curves of bacterial growth (Figure 4): strong suppression of bacterial growth (MF conjugates), plateau and/or decline of CFU for powerful antibacterial agents (MF and its non-covalent gel-formulations) is observed. For the samples (low concentrations of MF, and high concentrations of adjuvants components, EG, etc.): cells growth slows down. Finally: the effect is hardly noticeable (for chitosan, non-covalent formulation of linalool and limonene).

Among the individual components of terpenoids and allylbenzenes, the most effective was EG against *E. coli*, as well as EG, limonene and apiol against *B. Subtilis*. In addition, EG and its analogues demonstrate an amplifying effect for MF (Table 2) by 10-15% in terms of CFU (cell viability), which is potentially applicable to reduce the dose of toxic antibiotics.
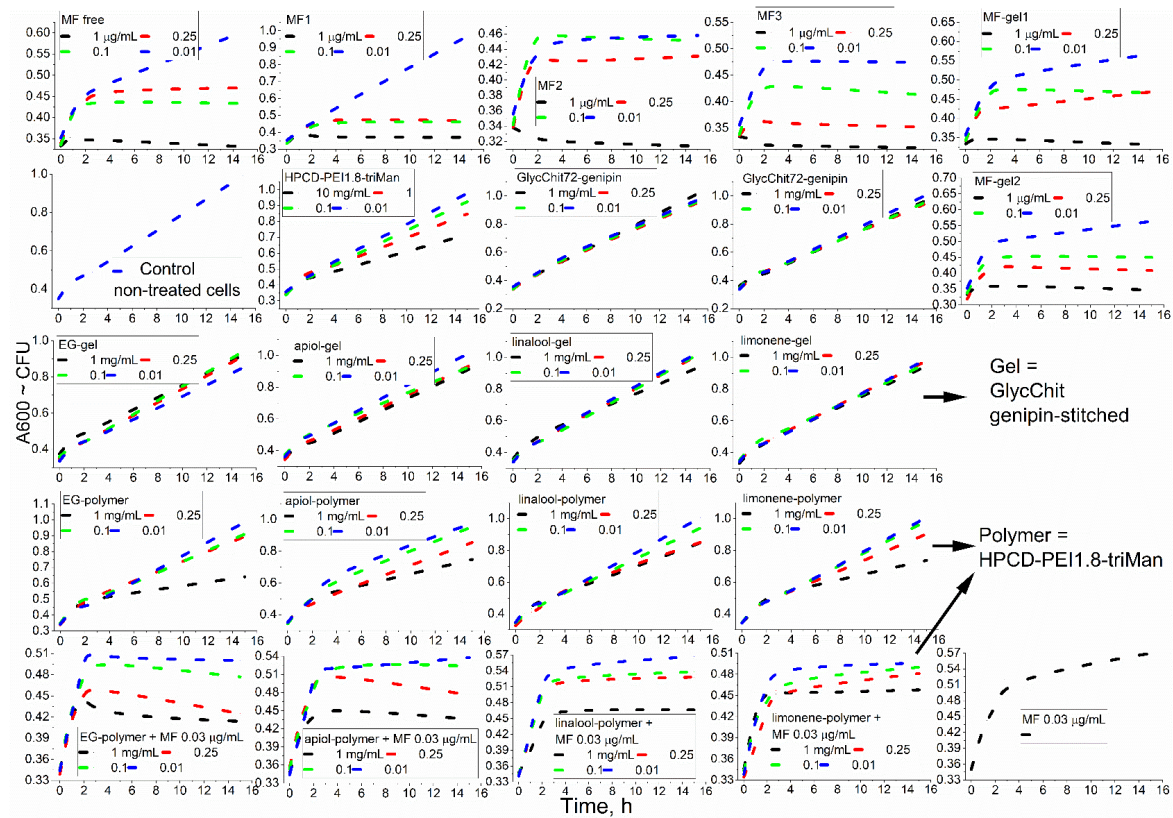
Figure 4. Kinetic curves of the dependence of the optical density at 600 nm, correlating with the number of colony-forming units, on the incubation time (0-16 h) of *E. coli* cells with antibacterial drugs. 37 °C. Line 3: gel is GlycChit genipin-stitched. Lines 4, 5: polymer = HPCD-PEI1.8-triMan. MF-gel1 = MF + GlycChit genipin-stitched. MF-gel2 = MF + GlycChit-acetylcysteine S-S stitched.

Table 1. The concentration of drug required for 50% inhibition of cell growth (IC50) of antibacterial formulations of Moxifloxacin. MF:polymer mass ratio = 3:1.

Designation	Chemical Composition	IC50 against *E. coli*, ng/mL	IC50 against *B. subtilis*, ng/mL
MF	MF free	8±2	800±300
MF1	MF-HPCD-PEI1.8-triMan	40±7	11±3
MF2	MF-GlycChit	4±1	9±2
MF3	MF-Mannan	3±1	10±3
MF-gel1	MF + GlycChit genipin-stitched	7±2	20±5
MF-gel2	MF + GlycChit-acetylcysteine S-S stitched	7±2	15±4

Table 2. Cell viability (as a percentage of CFU from control determined by DAPI cell staining) for formulation based on allylbenzenes, terpenes and terpenoids. Concentration of EG, apiol, linalool, limonene is 1 mg/mL.

Compound **X**	*E. coli*			*B. subtilis*		
	X-covalent with HPCD-PEI1.8-triMan (X-polymer)	MF free 30 ng/mL* + **X**-covalent with HPCD-PEI1.8-triMan	**X** + GlycChit genipin-stitched (X-gel)	**X**-covalent with HPCD-PEI1.8-triMan (X-polymer)	MF free 30 ng/mL**+ **X**-covalent with HPCD-PEI1.8-triMan	**X** + GlycChit genipin-stitched (X-gel)
EG	64±7	41±3	85±11	81±8	60±7	94±3
Apiol	75±9	44±5	92±8	81±7	59±7	93±4
Linalool	85±6	47±4	93±7	85±9	62±5	97±2
Limonene	74±9	46±2	94±5	83±6	59±7	89±5

*For free MF 30 ng/mL 57% cell viability is observed; ** For free MF 30 ng/mL 75% cell viability is observed.

Polymers themselves have a weak antibacterial effect (Figure 4, line 2), the strongest is characteristic of the PEI-containing polymer. Covalent conjugates of MF with polymers (Figure 4, line 1), as well as components of essential oils with polymers (Figure 4, line 4), turned out to be more active than non-covalent chitosan-based "gels" (Figure 4, MF-gel1, MF-gel2 and line 3). However, using nanogels formulation it is possible to achieve prolonged release of antibacterial drugs without modification of the drug itself. We have previously shown that the formation of chitosan particles is accompanied by the inclusion of hydrophobic substances, the delivery of which to bacteria will be improved due to high concentration and adsorption on the cell membrane. Thus, cross-linked polymers ("chitosan nanogels") have the potential for the delivery of antibacterial drugs composition.

2.2.2. Prolonged antibacterial experiment with the most promising formulations

After extensive screening, for prolonged "antibacterial experiment" we selected covalent (with higher antibacterial activity) and MF or linalool non-covalent formulations HPCD-PEI1.8-triMan for comparison. Figure 5 shows the dependences of survival (determined by A600 and DAPI staining dead cells methodic [63]) with additional control with seeding on Petri dishes) of gram-positive and gram-negative cells on the incubation time with antibacterial agents. We have observed that MF free and MF non-covalently included in the polymer nanogel inhibits cell growth, but not completely, and the bacteria continue to grow. We specially used such a concentration of MF to differentiate the observed effects. MF-HPCD-PEI1.8-triMan conjugate was found to be the most effective against both types of bacteria. Limonene in free form has a weak inhibitory effect on cell growth and can be used to enhance the antibiotic in the form of a covalent conjugate, which has shown excellent results in combination with covalently MF-prodrag (Figure 5b).

MF does not act more than 2-3 days, then a significant growth of bacteria is observed again (Figure 5a). At the same time, MF in the composition of conjugates, as well as enhanced with the adjuvant limonene, suppresses the growth of *E. coli* (up to 5% cell viability) and *B. subtilis* (completely). MF degrades after 2-3 days of incubation in an environment with cells that secrete enzymes [1]: MF biodegradation is associated with the elimination of the antibacterial properties of MF, even may lead to the development of resistant bacterial strains.
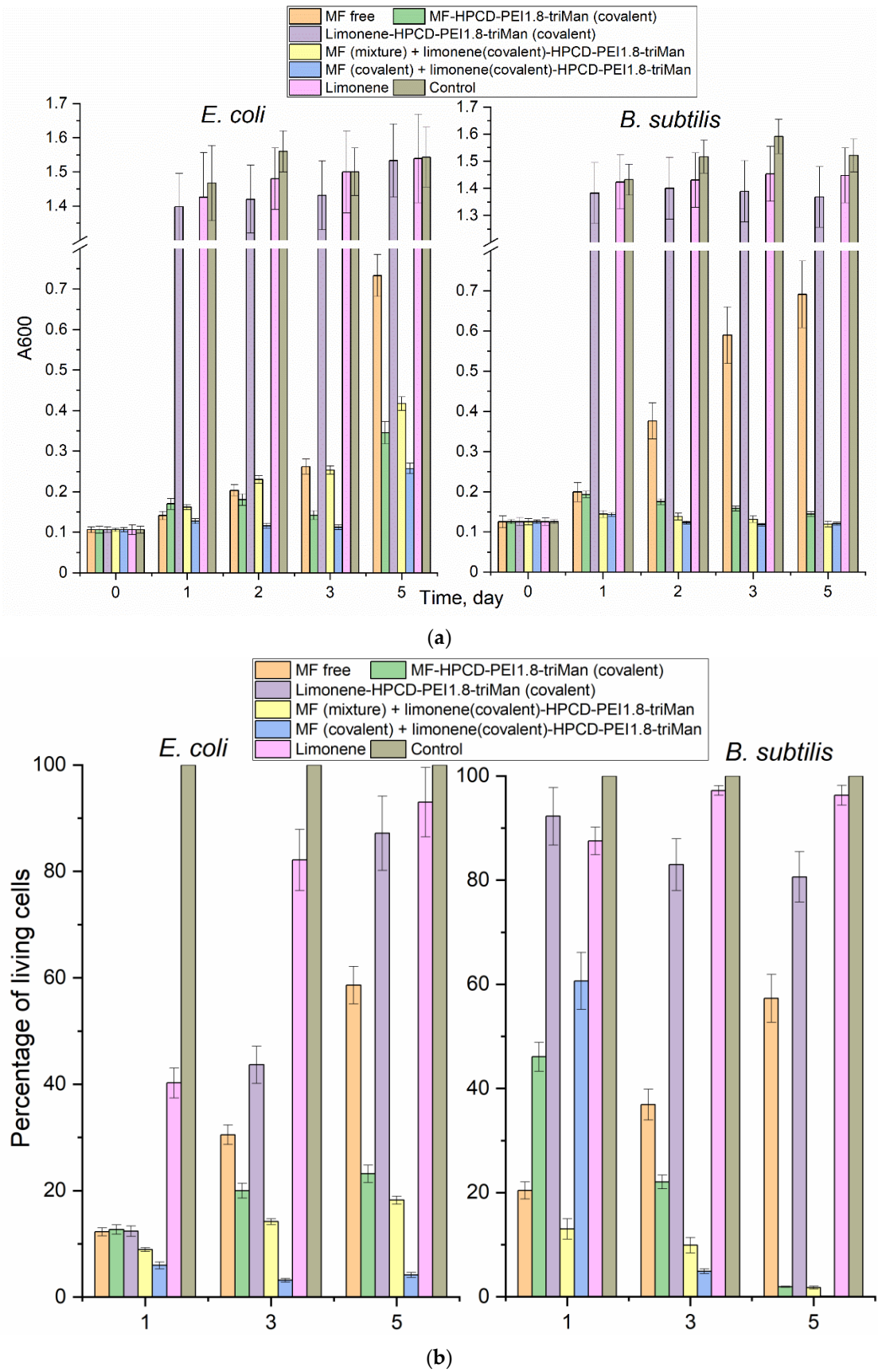
Figure 5. (a) The dependences of the optical density at 600 nm, correlating with the number of colony-forming units, on the incubation time of *E. coli* and *B. subtilis* cells with antibacterial drugs. **(b)** Staining of mostly dead bacterial cells by DAPI. C(MF) = 0.03 μg/mL. C(limonene) = 0.25 mg/mL. 37 °C.

2.3. FTIR spectroscopy as a tool for tracking drug penetration into cells and its effectiveness

We have shown the effectiveness of covalent conjugates in comparison with non-covalent ones; therefore it is necessary to show which mechanisms (factors) cause an increase in antibacterial activity. FTIR spectroscopy provides valuable information about molecular details of drug interactions with cells. The main structural units of cell are characterize by peaks in FTIR spectra: cell membrane lipids (2800–3000 cm^{-1}), proteins, especially transmembrane (1500–1700 cm^{-1}), DNA phosphate groups (1240 cm^{-1}), carbohydrates, including lipopolysaccharides (900–1100 cm^{-1}) [32]. The main oscillations of bonds in the structural units of *E. coli* cells: 2960–2850 cm^{-1} CH, CH$_2$, CH$_3$ in fatty acids, 1655–1637 cm^{-1} amide I bands (α-helical and β-pleated sheet structures), 1548 cm^{-1} amide II band, 1515 cm^{-1} aromatic band, 1465–1470 C–H deformation, 1310–1240 cm^{-1} amide III band components of proteins, 1250–1220 and 1084–1088 cm^{-1} P=O stretching of PO$_2^-$ − phosphodiesters, 1100–900 cm^{-1} C–O–C, C–O of saccharide ring vibrations [64].

Moxifloxacin is characterized by an intense band at 1454 cm^{-1}, corresponding to valence oscillations of C=C of the aromatic system sensitive to microenvironment. When adsorption on the cell surface or penetration inside, an increase in this peak is expected. Figure 6 shows the FTIR spectra of *E. coli* incubated with MF containing formulations and polymer. The interaction of MF with cell components (proteins, lipids in the membrane, oligosaccharides on the surface) leads to an increase in the intensity of peaks. The most striking changes in the penetration of MF and polymer adsorption occur in the bands of amide I and amid II, which characterize proteins. In addition, the peak selective to MF is at 1545 cm^{-1}, which shows practically only the MF state. The graphs (Figure 6f) show the critical dependences of the intensity of MF-peaks in the spectrum on the incubation time as a direct indicator of the effectiveness of drug accumulation in the cell. The changes in the amide I and amide II bands are greatest for unconjugated MF due to its high molecular mobility. The obtained results are consistent with microbiological data: the covalent conjugate with MF (HPCD-PEI1.8-triMan with amide bond) turned out to be the most effective, and an additional increase in penetration into the cell can be achieved by adding the adjuvant eugenol and other allylbenzenes and terpenoids (a similar effect is observed) as permeability enhancer and efflux inhibitors.
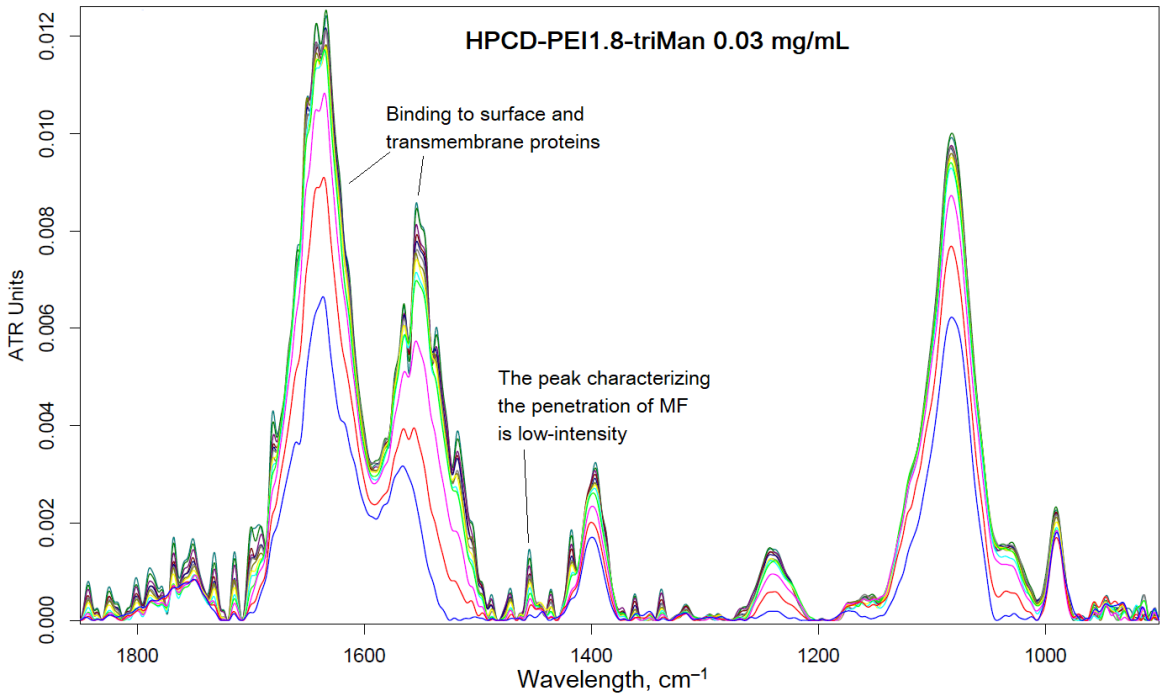
Thus, using FTIR spectroscopy, the high molecular mobility of free MF and its interaction with proteins is shown. At the same time, due to the adsorption of the polymer on the cell membrane and the high local concentration of MF on the polymer, the penetration of MF into the cells increases.
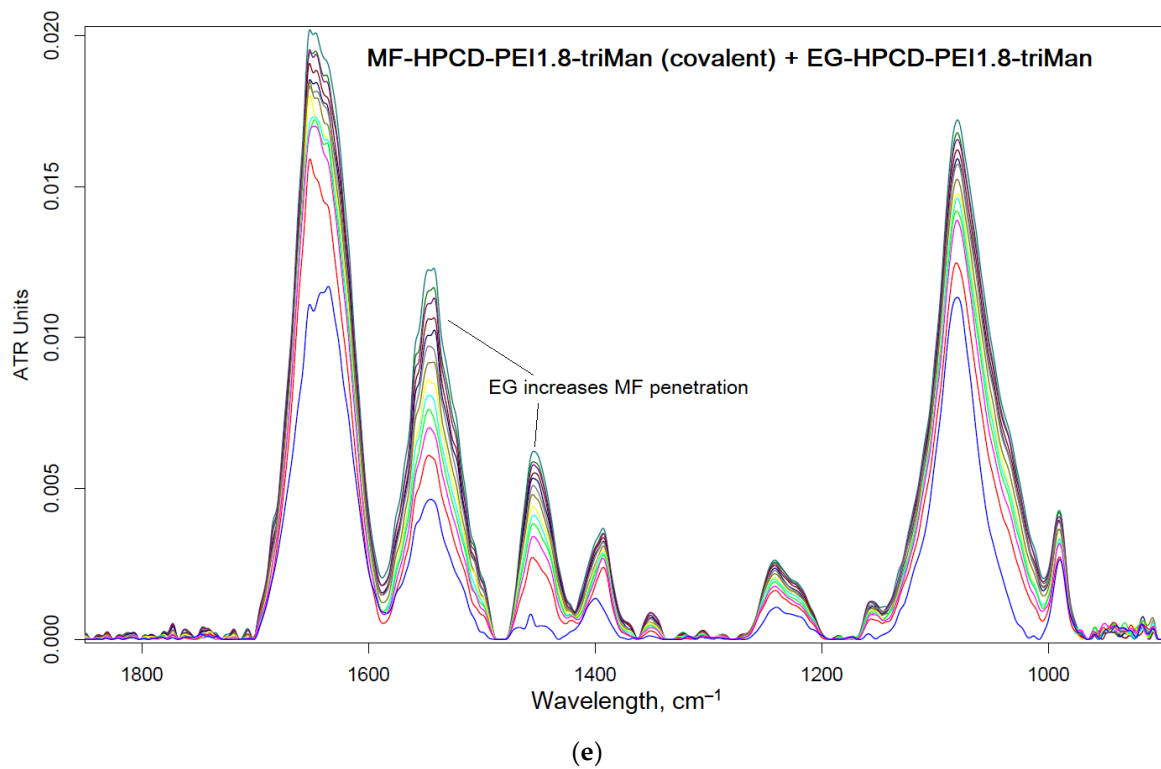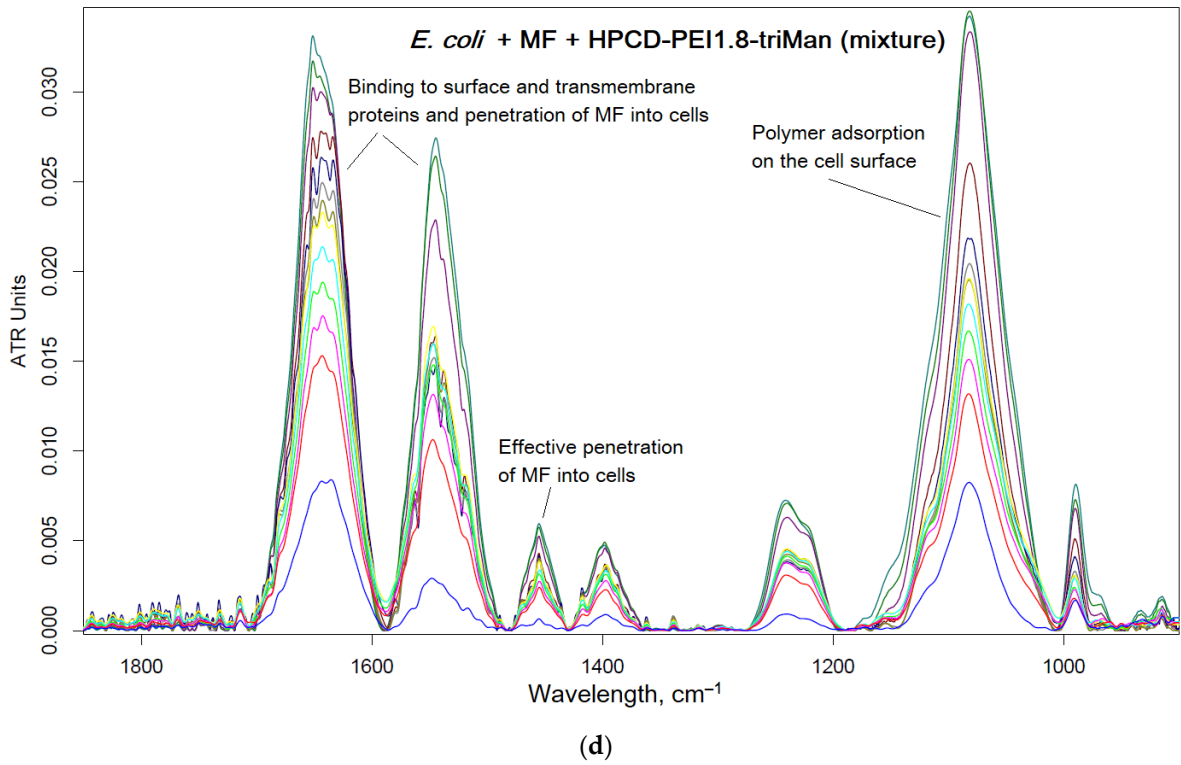

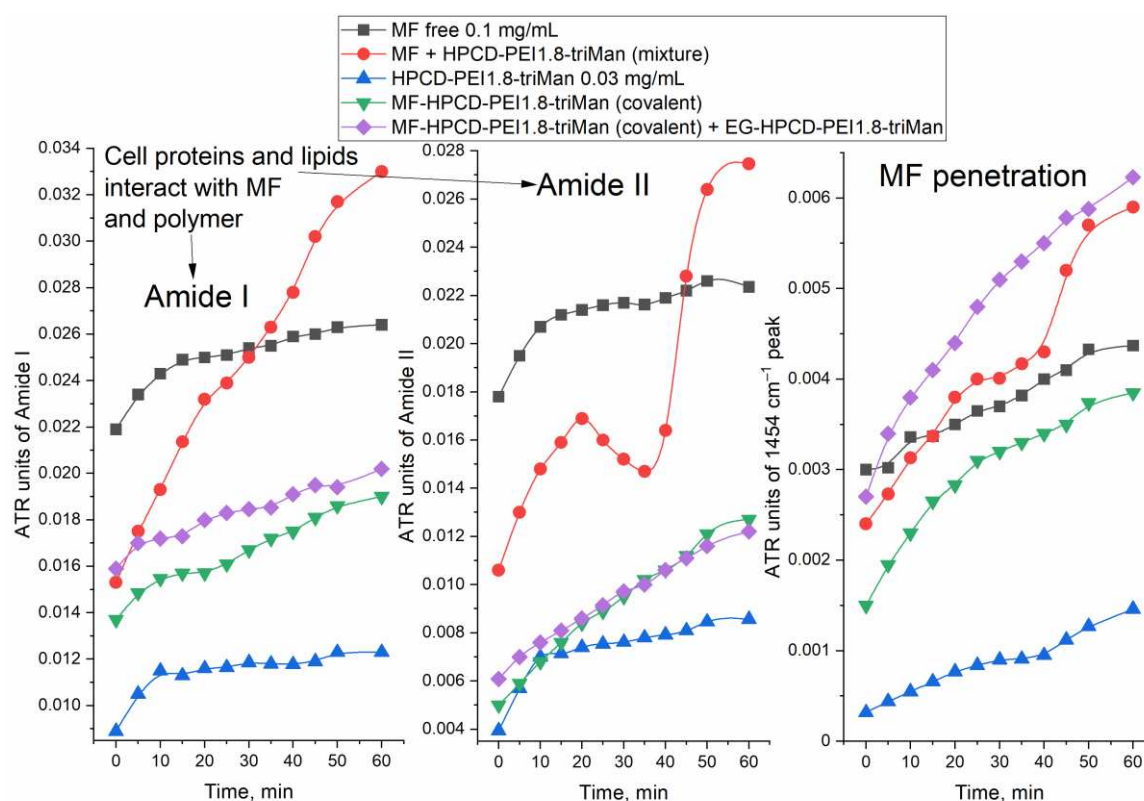**(a)**

(b)

(c)

(d)

(e)
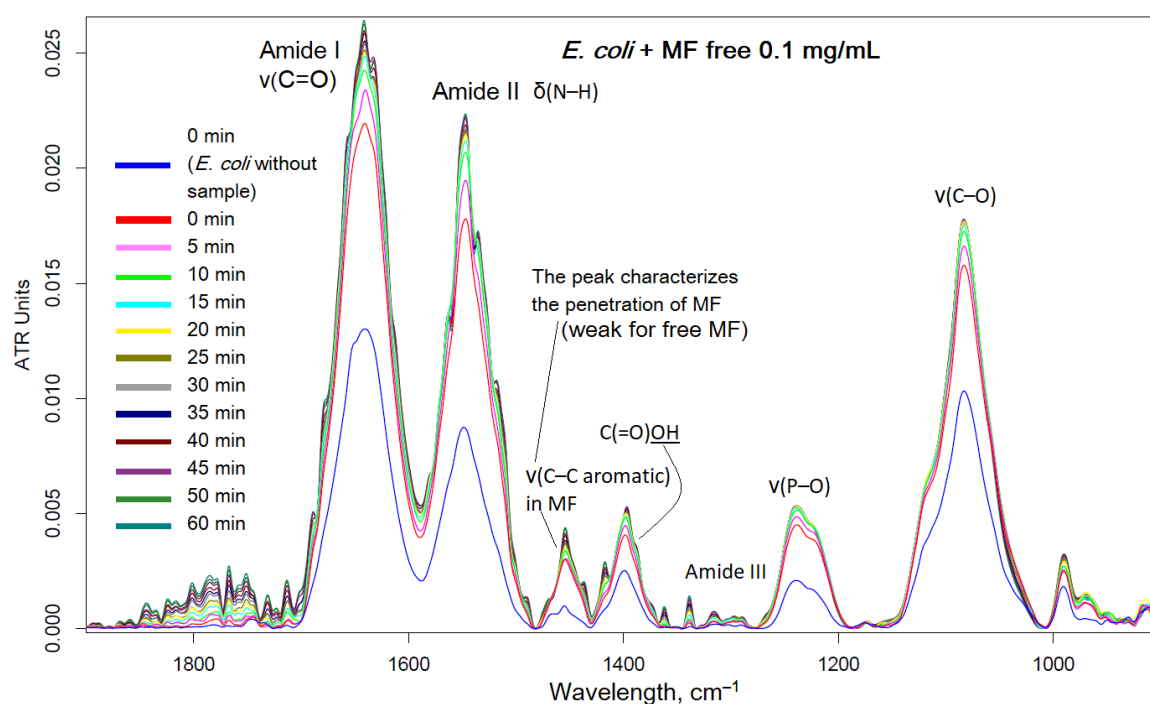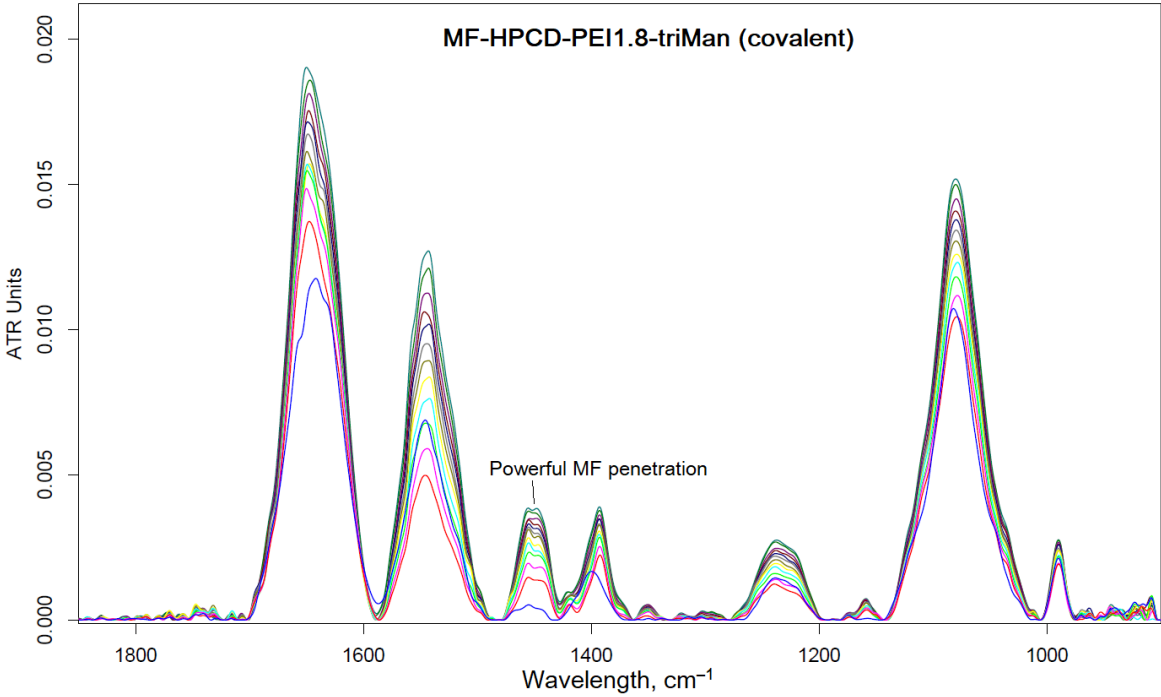
(**f**)

Figure 6. FTIR spectra of *E. coli* cells suspension in PBS during incubation at 37 °C with: (a) MF free, (b) MF-HPCD-PEI1.8-triMan, (c) HPCD-PEI1.8-triMan, (d) mixture of MF with HPCD-PEI1.8-triMan, (e) MF-HPCD-PEI1.8-triMan and EG-HPCD-PEI1.8-triMan. C(MF) = 0.1 mg/mL. C(polymer) = 0.03 mg/mL. C(EG) = 1 mg/mL. The color designations are similar for (a)-(e) figures and correspond to those shown on (a). (f) The corresponding dependences of the intensity of the FTIR peaks on the incubation time for different samples.

Thus, the most active was the covalent formulation of MF-HPCD-PEI1.8-triMan with the addition of adjuvants (EG and analogues conjugate with polymers), less active were non-covalent prodrugs based on MF and chitosan nanogels.

2.4. FTIR spectroscopy as a tool for determining the number of cells in antibacterial experiments

Above, we showed the applicability of FTIR spectroscopy to monitor the passage of a drug into a cell and found out the molecular details of the polymer's action. Here, we aimed to present FTIR spectroscopy from the other side – as a means of measuring the number of cells in antibacterial experiments and studying the state of cells by their structural elements. Figure 7 shows the FTIR spectra of bacteria recorded after 1 day of incubation with anti-bacterial drugs – a prolonged experiment (paragraph 2.2.2). In the case of *E. coli* for MF-HPCD-PEI1.8-triMan after centrifugation, we do not observe intact cells (blue curve, PBS spectrum, no intact cells). A small number of cells grew in the presence of MF free and a mixture of MF with polymer. Conjugation of limonene significantly enhances its (MF and adjuvant) antibacterial effect due to the positive charge of the polymer, as well as the high local concentration of the adjuvant. In case of *B. subtilis* similar pattern is observed, however, complete inhibition is not achieved after 1 day, although MF-HPCD-PEI1.8-triMan is also the best sample. The MF conjugate is enhanced by limonene in the conjugate, which is reflected in the intensity of the peak of amide 2 (Figure 7). The number of cells (according to the intensity of amide 2) correspond to antibacterial data (Figure 5).
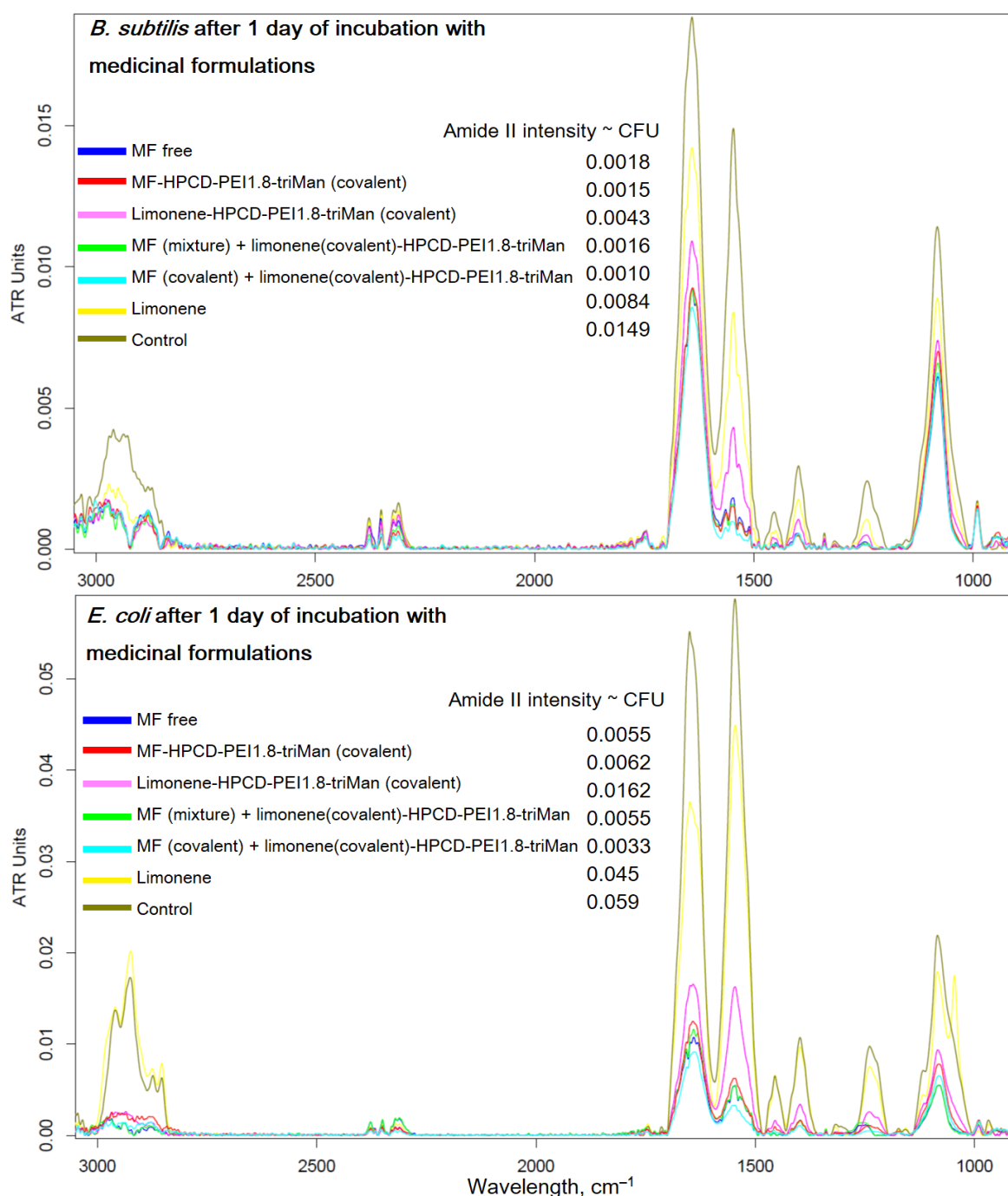
Figure 7. FTIR spectra of *E. coli* and *B. subtilis* cells suspensions in PBS after 1 day of incubation at 37 °C with samples similar to those used in the experiment described in Figure 5.

Therefore, FTIR is an highly informative method for monitoring the interaction of drugs with individual components of cells (Figure 7): polymers are adsorbed on the cell surface. at the same time increasing the efficiency of MF penetration inside. In addition, FTIR makes it possible to evaluate the effectiveness of antibacterial formulations in time due to direct control of the number of cells.

2.5. Pharmacokinetics of MF in polymer particles and covalent conjugates

An important use of essential oil components (EG, apiol, linalool and limonene) is their ability to influence the pharmacokinetics of an antibacterial drug. this is especially noticeable for covalent conjugates. The second aspect is the comparison of non-covalent and covalent MF formulations. Figure 8 shows the pharmacokinetic curves of MF concentration in rat blood plasma. Table 3 shows

the corresponding pharmacokinetic parameters using the two-compartment model. In all formulations of MF, the circulation time of MF increases and clearance decreases, while the greatest effect is achieved for the covalent conjugate of MF-mannan and MF included in cyclodextrins as part of HPCD-PEI1.8-triMan, enhanced with apiol, which inhibits a family of enzymes, including Cytochromes P450, which metabolize drugs [65–67].
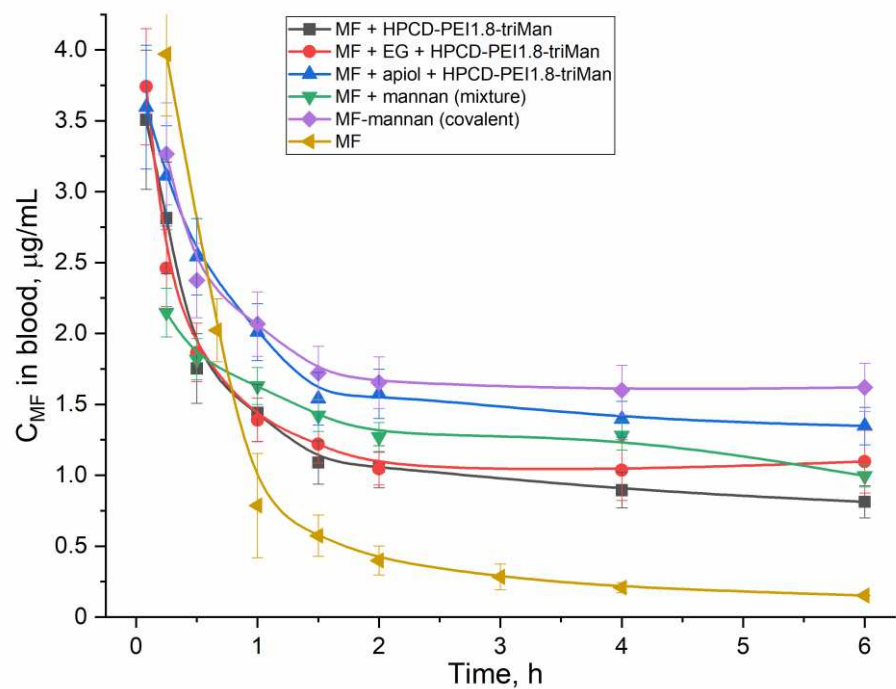
Figure 8. Pharmacokinetic curves of MF and its compositions with polymers (covalent and non-covalent forms) enhanced with adjuvants (EG, apiol) in white mongrel rats.

Table 3. Pharmacokinetic parameters of MF in white mongrel rats. Drugged animals. The study time is 6 h. Two-compartment model without absorption.

Parameters	MF Free	MF + HPCD-PEI1.8-triMan (Non-Covalent)	MF + EG + HPCD-PEI1.8-triMan (Non-Covalent)	MF + apiol + HPCD-PEI1.8-triMan (Non-Covalent)	MF-Mannan (Covalent)	MF + Mannan (Mixture)
Half-distribution period, min	20±2	15±1	12±2	25±4	15±2	14±2
Half-elimination period, h	6,5±0,5	10±1	22±2	45±6	42±7	24±3
Kinetical distribution volume, L	8±1	4±1	4±1	3±1	3±1	3±1
Stationary distribution volume, L	4±1	4±1	4±1	3±1	3±1	3±1
Clirens, mL/min	14±2	4,5±0,6	2,0±0,4	0,9±0,2	0,8±0,1	1,3±0,3
Area under curve	360±70	1100±200	2400±300	5800±700	6500±900	3800±500
Mean residence time, h	5±1	14±2	28±4	35±6	35±4	29±3

3. Materials and Methods

3.1. Reagents

Glycol chitosan 72 kDa (GlycChit, the degree of deacetylation is 92), mannan (46 kDa), polyethyleneimine 1.8 kDa (PEI1.8), Et2O, DMF, DMSO, HBr, (HOCH2CH2)3N, 2-hydroxypropyl-β-cyclodextrin (HPCD), 4-toluenesulfonyl chloride (TsCl), genipin, 1-Ethyl-3-(3-dimethylaminopropyl) carbodiimide (EDC), N-hydroxysuccinimide (NHS), N-acetylcysteine, limonene were purchased from Sigma Aldrich (St. Louis, MI, USA). Mannotriose-di-(N-acetyl-D-glucosamine) (triMan-GlcNAc2) was obtained from Dayang Chem (Hangzhou) Co., Ltd.

By CD spectroscopy (Jasco J-815 CD Spectrometer, Japan), the degree of deacylation in glycol-chitosan samples was determined by the peak at 215 nm corresponding to the absorption of the amide bond and it was 92%.

Moxifloxacin hydrochloride (MF) was obtained by Canon Pharma (Moscow, Russia).

Linalool was purchased from Rotichrom GC (Germany). Eugenol at the highest commercial quality were purchased from Acros Organics (Belgium). Apiol with 98-99% purity were obtained by high-efficiency distillation using a pilot plant device at N.D. Zelinsky Institute of Organic Chemistry RAS (Moscow, Russia) [42].

Components for LB medium were bactotrypton, agarose and yeast extract (Helicon, Russia), NaCl.

3.2. HPCD-PEI1.8-triMan polymer synthesis and properties

Activated HPCD was obtained as described earlier [6,63] by reaction of HPCD OH-groups with carbonyldiimidazole in DMSO. 100 mg of PEI1.8 and 200 mg of triMan-GlcNAc2 were mixed followed by dissolution in 10 mL of 10 mM HCl. NaOH was added to the sample to achieve pH 6-7 and NaBH3CN to reduce Schiff base. The mixture was incubated at 70 °C for 48 hours. Then, 5-fold molar (on PEI1.8) excess of activated HPCD was added to the mixture followed by incubation at 70 °C for 24 hours. Polymer purification was carried out by dialysis against water for 24 h with water replacement (cut-off 3.5 kDa) and centrifugation (cut-off 3 kDa). Polymer was freeze-dried at –60°C (Edwards 5, BOC Edwards, UK). The purification of the sample was performed by HPLC gel filtration as described earlier [63]. The degree of mannosylation and HPCD-grafting was calculated according to spectrophotometric titration of amino groups (before and after reaction) with 2,4,6-trinitrobenzenesulfonic acid [6,17] and FTIR and NMR data. Mainly, primary amino groups were detected.

Polymer properties: HPCD-PEI1.8-triMan is characterize by molecular weight 10±3 kDa with corresponding molar ratio of components 3:1:5, hydrodynamic size 120±30 nm, zeta potential +5±1 mV.

3.3. MF conjugation with polymers

We used HPCD-PEI1.8-triMan, glycol-chitosan (GlycChit), and mannan to obtain covalent conjugates with MF (MF1-MF3).

MF1. The synthesis was carried out based on the reaction (Figure 1) described by the authors [68]. 130 mg of MF was mixed with EDC (150 mg) and NHS (65 mg), dissolved in 15 ml of PBS (0.01M, pH 7.4). The mixture was incubated for 30 min at 70 °C. Then 45 mg HPCD-PEI1.8-triMan was added and 20 h stirred at at 70 °C. Conjugate purification was carried out by dialysis against water for 24 h with water replacement (cut-off 6-8 kDa) and centrifugation (cut-off 10 kDa).

MF2 and MF3. The synthesis was carried out based on the reaction (Figure 1b) described in the works with modification [69,70]. MF (100 mg) was mixtured with TsCl (1.1 molar excess) and dissolved in 2 mL of DMF. The mixture was incubated for 1 hour at 80 C. Then glycol-chitosan (GlycChit) or mannan (25 mg) was added and incubated for another 24 hours at 80 C. After that, 1 ml of Et2O was added to the cooled solutions to precipitate the product. Et2O was evaporated followed by dissolution in water and centrifugation (cut-off 10 kDa).

The content of MF in all samples is determined by A280. The samples are frozen and freeze-dried as described in paragraph 3.2.

3.4. MF non-concovalent formulations obtaining

MF-gel1. 20 mg of MF was mixed with 7 mg of GlycChit and 0.5 mg of genipin was added. The mixture was dissolved in 3 ml of PBS and incubated for 24 hours at 60 C. Genipin stitches chitosan chains as shown in works [45–50,71] and loads MF molecules.

MF-gel2. 40 mg of GlyChit modified 110 mg of N-acetylcysteine similarly to the described for MF1. GlycChit-ACC was mixed with MF in a mass ratio of 1:3 with subsequent incubation at 50 °C in PBS for 2 hours after the addition of 5 mg oxidized glutathione for S-S crosslinking of GlycChit-ACC chains.

Using an atomic force microscope (AFM microscope INTEGRA II), the particle sizes of nanogels obtained by crosslinking with genipine and acetyl-cysteine were controlled: 200-350 nm.

3.5. Adjuvant conjugation with polymers

0.5 mL of HBr (48%) was added to 0.1 g of eugenol (EG), apiol, linalool, limonene [15]. The mixture was incubated for a day at 50 °C. 0.5 mL Et_2O and 0.5 mL H_2O were added to the cooled solution for extraction. The ether from the extract was evaporated and then HPCD-PEI1.8-triMan (polymer/adjuvant = 1:5 w/w) was added to the Br-modified substances in PBS, the samples were incubated at 70 °C for 12 hours. Conjugate purification was carried out by centrifugation (cut-off 10 kDa).

3.6. FTIR Spectroscopy

FTIR spectra of samples were recorded using a Bruker Tensor27 spectrometer equipped with a liquid nitrogen-cooled MCT (mercury cadmium telluride) detector, as described earlier [6,32,72,73].

3.7. NMR Spectroscopy

10-15 mg of the samples were dissolved in 700 μL of D_2O. ^1H NMR spectra of the solutions were recorded on a Bruker Avance 400 spectrometer (Germany) with an operating frequency of 400 MHz. Chemical shifts are given in ppm on the δ scale relative to hexamethyldisiloxane as an internal standard. The analysis and processing of NMR spectra were performed in the program MestReNova v.12.0.0–20080 (Mestrelab Research S.L.).

3.8. Antibacterial activity studies: FTIR spectoscopy, microbiology

The strains used in this study were *Escherichia coli* (ATCC 25922) and *Bacillus subtilis* (ATCC 6633) from National Resource Center Russian collection of industrial microorganisms SIC "Kurchatov Institute"). The culture was cultivated for 18-20 h at 37 °C to CFU/mL $\approx 10^7$ (determined by A_{600}) in liquid nutrient medium Luria-Bertani (pH 7.2): *E. coli* - without stirring, *B. subtilis* – with stirring 100 rpm.

ATR-FTIR spectra of cells samples suspension were recorded using followed procedure: overnight cell suspensions (10^7 CFU/mL) were washed twice with sterile PBS (pH 7.4) from the culture medium by centrifuging (Eppendorf centrifuge 5415C, 5 min, 10,000×g). The cells are precipitated by centrifugation and separated from the supernatant, washed twice and resuspended in PBS (10^8 cells/mL) to register FTIR spectra. Cell suspensions were incubated with MF-containing samples and FTIR spectra were registered at 37 °C online.

Microbiologic studies. The culture was cultivated for 18–20 h at 37 °C to CFU $\approx 0.3 \times 10^8$ (colony-forming unit) in liquid nutrient medium Luria–Bertani (pH 7.2). The experiments in liquid media were conducted by adding 50 μL of the samples to the 5000 μL of cell culture. The specimens were incubated at 37 °C for seven days. At the specific time, 300 μL of each sample was taken, diluted with PBS, and the absorbance was measured at 600 nm (with CFU control). For quantitative analysis of the dependences of CFU (cell viability) on the concentration of MF 50 μL of each sample was diluted 10^6–

10^8 times and seeded on the Petri dish. Dishes were placed in the incubator at 37 °C for 24 h. Then the number of the colonies (CFU) was counted. The number of living cells was additionally determined by the fluorescence of the DAPI dye relative to obviously dead cells and living ones after 10 minutes incubation of 200 μL of a cell suspension sample with 1 μg/mL of DAPI.

4. Conclusions

Natural extracts from essential oils: allylbenzenes, terpenes, terpenoids are important biologically active substances that are promising in the aspects of creating new enhanced antibacterial and antitumor formulations. In this work, EG, apiol, linalool and limonene were studied as enhancers of the action of fluoroquinolone MF against *E.coli* and *B.subtilis*. We have obtained MF-prodrug (covalent formulations) and adjuvants with polymers based on PEI, cyclodextrins, chitosan and mannan, as well as nanogels that include drug formulations due to crosslinking of the polymer chains directly, so as not to modify the drug functional groups. Polymer-MF demonstrated an increase in the antibacterial effect of MF with a decrease in the minimum inhibitory concentration by 2-5 times, an increase in the penetration of MF into cells, as well as a prolonged duration of more than 5 days (versus 1-3 for simple MF). We have presented an original technique for tracking the interaction of a drug and a delivery system with bacterial cells using FTIR spectroscopy, which provides valuable information about the structural components of the cell. So, we have shown that adjuvant-polymer (covalent formulations) increase the MF influx due to the action as a membrane permeability enhancer and efflux inhibitors. Covalent conjugates, as well as polymer particles with the addition of apiol (cytochrome P450 inhibitor) improve the pharmacokinetic parameters of MF: the half-life increases by 6-8 times, while the area under the kinetic curve, which characterizes the effective concentration of the drug, increased by more than 10 times. Thus, covalent formulations of MF and adjuvants (terpenoids and allylbenzenes) have the potential in terms of the construction of drugs with the function of overcoming multidrug resistance and long-term action.

Author Contributions: Conceptualization, I.D.Z. and E.V.K.; methodology, I.D.Z. and E.V.K.; software, S.S.K., M.R.D., M.P.D., N.G.B.; formal analysis, I.D.Z.; investigation, I.D.Z., M.R.D., M.P.D., S.S.K.; data curation, I.D.Z., E.V.K.; writing—original draft preparation, I.D.Z.; writing—review and editing, E.V.K., I.D.Z., N.G.B.; project administration, E.V.K.; funding acquisition, E.V.K. All authors have read and agreed to the published version of the manuscript.

Abbreviations

EG	eugenol
GlycChit	glycol chitosan
HPCD	(2-hydroxypropyl)-β-cyclodextrin
IC50	half maximal inhibitory concentration
MF	moxifloxacin
PEI	polyethyleneimine
triMan	mannotriose residue

Appendix A

(**a**)

(**b**)

(c)
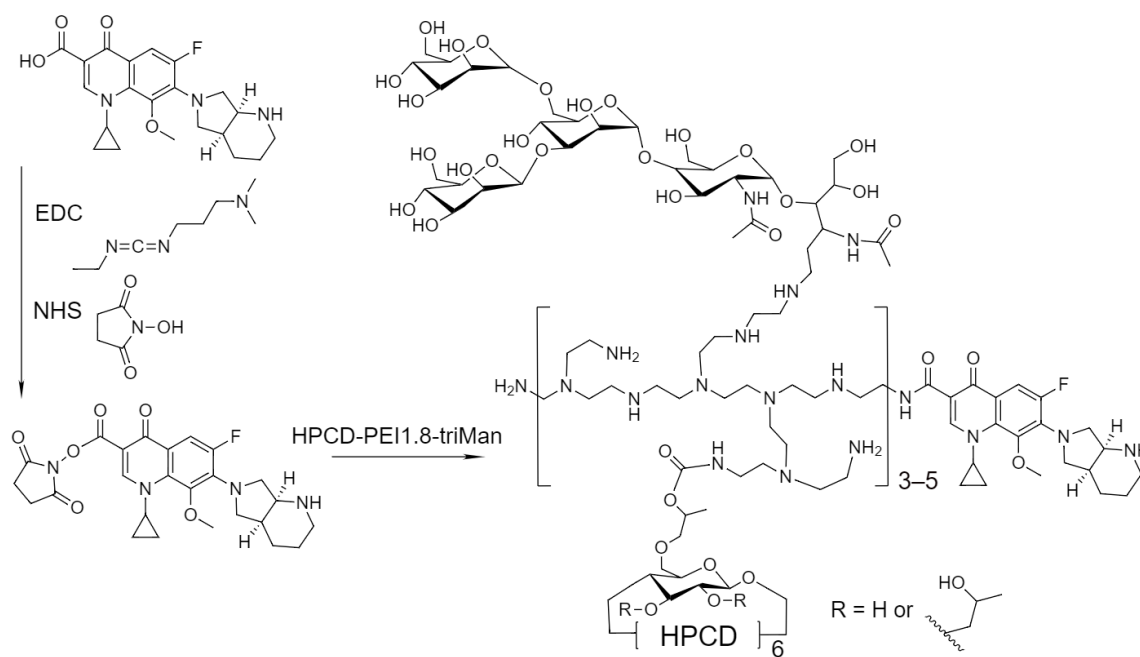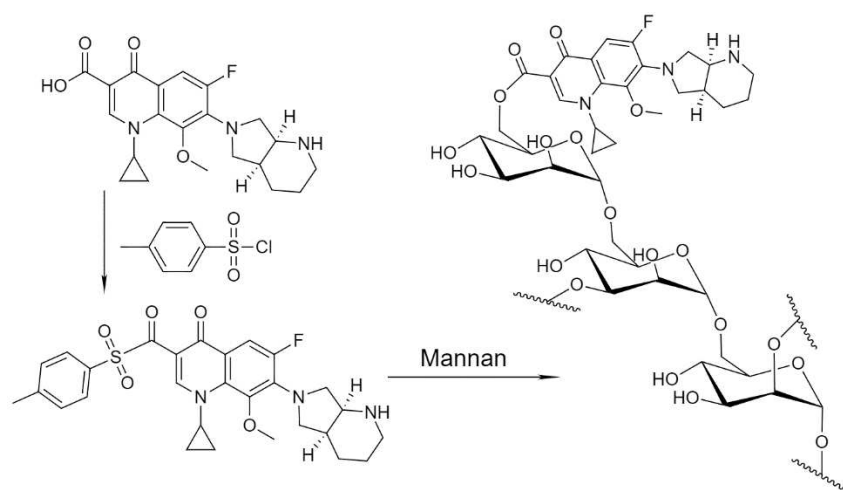
Figure A1. The scheme of synthesis of conjugates MF-polymer based on: (a) HPCD-PEI1.8-triMan, (b) GlycChit, (c) Mannan.

References

1. Carvalho, M.F.; Maia, A.S.; Tiritan, M.E.; Castro, P.M.L. Bacterial degradation of moxifloxacin in the presence of acetate as a bulk substrate. *J. Environ. Manage.* **2016**, *168*, 219–228, doi:10.1016/j.jenvman.2015.12.010.
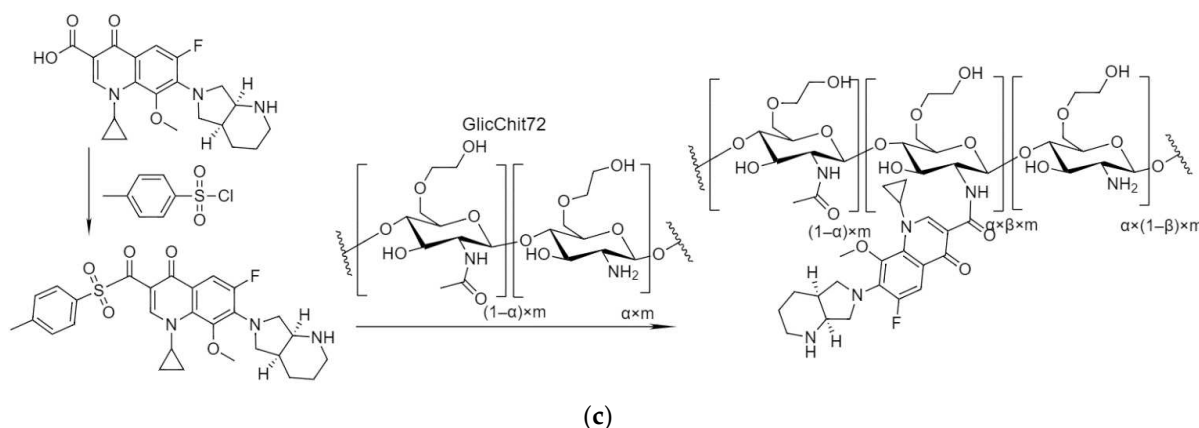2. Tejashri, G.; Amrita, B.; Darshana, J. Cyclodextrin based nanosponges for pharmaceutical use: A review. *Acta Pharm.* **2013**, *63*, 335–358, doi:10.2478/acph-2013-0021.
3. Pereira, P.; Morgado, D.; Crepet, A.; David, L.; Gama, F.M. Glycol chitosan-based nanogel as a potential targetable carrier for siRNA. *Macromol. Biosci.* **2013**, *13*, 1369–1378, doi:10.1002/mabi.201300123.
4. Mohamed, S.H.; Arafa, A.S.; Mady, W.H.; Fahmy, H.A.; Omer, L.M.; Morsi, R.E. Preparation and immunological evaluation of inactivated avian influenza virus vaccine encapsulated in chitosan nanoparticles. *Biologicals* **2018**, *51*, 46–53, doi:10.1016/j.biologicals.2017.10.004.
5. Le-Deygen, I.M.; Skuredina, A.A.; Kudryashova, E. V. Drug delivery systems for fluoroquinolones: New prospects in tuberculosis treatment. *Russ. J. Bioorganic Chem.* **2017**, *43*, 487–501, doi:10.1134/S1068162017050077.
6. Zlotnikov, I.D.; Kudryashova, E. V Spectroscopy Approach for Highly - Efficient Screening of Lectin - Ligand Interactions in Application for Mannose Receptor and Molecular Containers for Antibacterial Drugs. **2022**.
7. Ghotbi, Z.; Haddadi, A.; Hamdy, S.; Hung, R.W.; Samuel, J.; Lavasanifar, A. Active targeting of dendritic cells with mannan-decorated PLGA nanoparticles. *J. Drug Target.* **2011**, *19*, 281–292, doi:10.3109/1061186X.2010.499463.
8. Ran, S.; Volk, L.; Hall, K.; Flister, M.J. Lymphangiogenesis and lymphatic metastasis in breast cancer. *Pathophysiology* **2010**, *17*, 229–251, doi:10.1016/j.pathophys.2009.11.003.
9. Hoffmann, S.; Gorzelanny, C.; Moerschbacher, B.; Goycoolea, F.M. Physicochemical characterization of FRET-labelled chitosan nanocapsules and model degradation studies. *Nanomaterials* **2018**, *8*, doi:10.3390/nano8100846.
10. Gheran, C.V.; Voicu, S.N.; Galateanu, B.; Callewaert, M.; Moreau, J.; Cadiou, C.; Chuburu, F.; Dinischiotu, A. In Vitro Studies Regarding the Safety of Chitosan and Hyaluronic Acid-Based Nanohydrogels Containing Contrast Agents for Magnetic Resonance Imaging. *Int. J. Mol. Sci.* **2022**, *23*, doi:10.3390/ijms23063258.
11. Gordon, S. The role of the macrophage in immune regulation. *Res. Immunol.* **1998**, *149*, 685–688, doi:10.1016/S0923-2494(99)80039-X.
12. Paczkowska-Walendowska, M.; Cielecka-Piontek, J. Chitosan as a Functional Carrier for the Local Delivery Anti-Inflammatory Systems Containing Scutellariae baicalensis radix Extract. *Pharmaceutics* **2022**, *14*, 1–14, doi:10.3390/pharmaceutics14102148.
13. n, Eunsung Mouradian, M.M. 基因的改变 NIH Public Access. *Bone* **2008**, *23*, 1–7, doi:10.1016/j.jconrel.2014.09.006.Optimal.

14.   Di Benedetto, P.; Ruscitti, P.; Vadasz, Z.; Toubi, E.; Giacomelli, R. Macrophages with regulatory functions, a possible new therapeutic perspective in autoimmune diseases. *Autoimmun. Rev.* **2019**, *18*, 102369, doi:10.1016/j.autrev.2019.102369.

15.   Serra, P.; Santamaria, P. Nanoparticle-based autoimmune disease therapy. *Clin. Immunol.* **2015**, *160*, 3–13, doi:10.1016/j.clim.2015.02.003.

16.   Sato, A.; Kawakami, S.; Yamada, M.; Yamashita, F.; Hashida, M. Enhanced gene transfection in macrophages using mannosylated cationic liposome-polyethylenimine-plasmid DNA complexes. *J. Drug Target.* **2001**, *9*, 201–207, doi:10.3109/10611860108997928.

17.   Le-Deygen, I.M.; Mamaeva, P. V.; Skuredina, A.A.; Kudryashova, E. V. A Spectral Approach to Study Interaction between Chitosan Modified with Mannose and Concavalin A for the Creation of Address Delivery Systems of Antituberculosis Drugs. *Moscow Univ. Chem. Bull.* **2020**, *75*, 213–217, doi:10.3103/S0027131420040045.

18.   Alizadeh, D.; Zhang, L.; Hwang, J.; Schluep, T.; Badie, B. Tumor-associated macrophages are predominant carriers of cyclodextrin-based nanoparticles into gliomas. *Nanomedicine Nanotechnology, Biol. Med.* **2010**, *6*, 382–390, doi:10.1016/j.nano.2009.10.001.

19.   Zlotnikov, I.D.; Vigovskiy, M.A.; Davydova, M.P.; Danilov, M.R.; Dyachkova, U.D.; Grigorieva, O.A.; Kudryashova, E. V Mannosylated Systems for Targeted Delivery of Antibacterial Drugs to Activated Macrophages. **2022**, 1–29.

20.   Raviv, L.; Jaron-Mendelson, M.; David, A. Mannosylated polyion complexes for in vivo gene delivery into CD11c+ dendritic cells. *Mol. Pharm.* **2015**, *12*, 453–462, doi:10.1021/mp5005492.

21.   Nahar, M.; Dubey, V.; Mishra, D.; Mishra, P.K.; Dube, A.; Jain, N.K. In vitro evaluation of surface functionalized gelatin nanoparticles for macrophage targeting in the therapy of visceral leishmaniasis . *J. Drug Target.* **2009**, *00*, 090729062238077–13, doi:10.1080/10611860903115290.

22.   Cho, K.; Wang, X.; Nie, S.; Chen, Z.; Shin, D.M. Therapeutic nanoparticles for drug delivery in cancer. *Clin. Cancer Res.* **2008**, *14*, 1310–1316, doi:10.1158/1078-0432.CCR-07-1441.

23.   Jain, S.; Attarwala, H. (12) United States Patent. **2019**, *2*.

24.   Piotrowski-Daspit, A.S.; Kauffman, A.C.; Bracaglia, L.G.; Saltzman, W.M. Polymeric vehicles for nucleic acid delivery. *Adv. Drug Deliv. Rev.* **2020**, *156*, 119–132, doi:10.1016/j.addr.2020.06.014.

25.   Gao, J.Q.; Zhao, Q.Q.; Lv, T.F.; Shuai, W.P.; Zhou, J.; Tang, G.P.; Liang, W.Q.; Tabata, Y.; Hu, Y.L. Gene-carried chitosan-linked-PEI induced high gene transfection efficiency with low toxicity and significant tumor-suppressive activity. *Int. J. Pharm.* **2010**, *387*, 286–294, doi:10.1016/j.ijpharm.2009.12.033.

26.   Qindeel, M.; Ahmed, N.; Khan, G.M.; Rehman, A. Ligand decorated chitosan as an advanced nanocarrier for targeted delivery: A critical review. *Nanomedicine* **2019**, *14*, 1623–1642, doi:10.2217/nnm-2018-0490.

27.   Mantovani, A.; Marchesi, F.; Malesci, A.; Laghi, L. Europe PMC Funders Group Tumor-Associated Macrophages as Treatment Targets in Oncology. **2018**, *14*, 399–416, doi:10.1038/nrclinonc.2016.217.Tumor-Associated.

28.   Zlotnikov, I.D.; Ezhov, A.A.; Petrov, R.A.; Vigovskiy, M.A.; Grigorieva, O.A.; Belogurova, N.G.; Kudryashova, E. V. Mannosylated Polymeric Ligands for Targeted Delivery of Antibacterials and Their Adjuvants to Macrophages for the Enhancement of the Drug Efficiency. *Pharmaceuticals* **2022**, *15*, 1172, doi:10.3390/ph15101172.

29.   Zlotnikov, I.D.; Vanichkin, D.A.; Kudryashova, E.V. Methods for Determining the Parameters of Receptor-Ligand Interactions on the Model of Concanavalin A and Mannosylated Chitosans Promising Carriers for Drug Delivery to Alveolar Macrophages. *Biotekhnologiya* **2021**, *37*, 28–40, doi:10.21519/0234-2758-2021-37-5-28-40.

30.   Zlotnikov, I.D.; Kudryashova, E. V. Mannose Receptors of Alveolar Macrophages as a Target for the Addressed Delivery of Medicines to the Lungs. *Russ. J. Bioorganic Chem.* **2022**, *48*, 46–75, doi:10.1134/S1068162022010150.

31.   Zlotnikov, I.D.; Kudryashova, E. V. Computer simulation of the Receptor–Ligand Interactions of Mannose Receptor CD206 in Comparison with the Lectin Concanavalin A Model. *Biochem.* **2022**, *87*, 54–69, doi:10.1134/S0006297922010059.

32.   Zlotnikov, I.D.; Ezhov, A.A.; Vigovskiy, M.A.; Grigorieva, O.A.; Dyachkova, U.D.; Belogurova, N.G.; Kudryashova, E. V Application Prospects of FTIR Spectroscopy and CLSM to Monitor the Drugs Interaction with Bacteria Cells Localized in Macrophages for Diagnosis and Treatment Control of Respiratory Diseases. **2023**, 1–23.

28

33. Bhat, A.R.; Wani, F.A.; Behera, K.; Khan, A.B.; Patel, R. Formulation of biocompatible microemulsions for encapsulation of anti-TB drug rifampicin: A physicochemical and spectroscopic study. *Colloids Surfaces A Physicochem. Eng. Asp.* **2022**, *645*, 128846, doi:10.1016/j.colsurfa.2022.128846.

34. Jafri, H.; Banerjee, G.; Khan, M.S.A.; Ahmad, I.; Abulreesh, H.H.; Althubiani, A.S. Synergistic interaction of eugenol and antimicrobial drugs in eradication of single and mixed biofilms of Candida albicans and Streptococcus mutans. *AMB Express* **2020**, *10*, doi:10.1186/s13568-020-01123-2.

35. Weisheimer, V.; Miron, D.; Silva, C.B.; Guterres, S.S.; Schapoval, E.E.S. Microparticles containing lemongrass volatile oil: Preparation, characterization and thermal stability. *Pharmazie* **2010**, *65*, 885–890, doi:10.1691/ph.2010.0139.

36. Leite, A.M.; Lima, E.D.O.; De Souza, E.L.; Diniz, M.D.F.F.M.; Trajano, V.N.; De Medeiros, I.A. Inhibitory effect of β-pinene, α-pinene and eugenol on the growth of potential infectious endocarditis causing Gram-positive bacteria. *Rev. Bras. Ciencias Farm. J. Pharm. Sci.* **2007**, *43*, 121–126, doi:10.1590/S1516-93322007000100015.

37. Tsyganov, D. V.; Samet, A. V.; Silyanova, E.A.; Ushkarov, V.I.; Varakutin, A.E.; Chernysheva, N.B.; Chuprov-Netochin, R.N.; Khomutov, A.A.; Volkova, A.S.; Leonov, S. V.; и др. Synthesis and Antiproliferative Activity of Triphenylphosphonium Derivatives of Natural Allylpolyalkoxybenzenes. *ACS Omega* **2022**, *7*, 3369–3383, doi:10.1021/acsomega.1c05515.

38. Elshafie, H.S.; Sakr, S.H.; Sadeek, S.A.; Camele, I. Biological Investigations and Spectroscopic Studies of New Moxifloxacin/Glycine-Metal Complexes. *Chem. Biodivers.* **2019**, *16*, doi:10.1002/cbdv.201800633.

39. Semenov, V. V.; Kiselyov, A.S.; Titov, I.Y.; Sagamanova, I.K.; Ikizalp, N.N.; Chernysheva, N.B.; Tsyganov, D. V.; Konyushkin, L.D.; Firgang, S.I.; Semenov, R. V.; и др. Synthesis of antimitotic polyalkoxyphenyl derivatives of combretastatin using plant allylpolyalkoxybenzenes (1). *J. Nat. Prod.* **2010**, *73*, 1796–1802, doi:10.1021/np1004278.

40. Kost, B.; Brzeziński, M.; Zimnicka, M.; Socka, M.; Wielgus, E.; Słowianek, M.; Biela, T. PLA Stereocomplexed Microspheres Modified with Methyl-β-Cyclodextrin as an Atropine Delivery System. Synthesis and Characterization. *Mater. Today Commun.* **2020**, *25*, doi:10.1016/j.mtcomm.2020.101605.

41. Pereira de Lira, M.H.; Fernandes Queiroga Moraes, G.; Macena Santos, G.; Patrício de Andrade Júnior, F.; De Oliveira Pereira, F.; Oliveira Lima, I. Synergistic antibacterial activity of monoterpenes in combination with conventional antimicrobials against Gram-positive and Gram-negative bacteria. *Rev. Ciências Médicas e Biológicas* **2020**, *19*, 258, doi:10.9771/cmbio.v19i2.33665.

42. Zlotnikov, I.D.; Belogurova, N.G.; Krylov, S.S.; Semenova, M.N.; Semenov, V. V; Kudryashova, E. V Plant Alkylbenzenes and Terpenoids in the Form of Cyclodextrin Inclusion Complexes as Antibacterial Agents and Levofloxacin Synergists. **2022**.

43. Tadtong, S.; Watthanachaiyingcharoen, R.; Kamkaen, N. Antimicrobial constituents and synergism effect of the essential oils from Cymbopogon citratus and Alpinia galanga. *Nat. Prod. Commun.* **2014**, *9*, 277–280, doi:10.1177/1934578x1400900237.

44. Cardoso, N.N.R.; Alviano, C.S.; Blank, A.F.; Romanos, M.T. V.; Fonseca, B.B.; Rozental, S.; Rodrigues, I.A.; Alviano, D.S. Synergism Effect of the Essential Oil from Ocimum basilicum var. Maria Bonita and Its Major Components with Fluconazole and Its Influence on Ergosterol Biosynthesis. *Evidence-based Complement. Altern. Med.* **2016**, *2016*, doi:10.1155/2016/5647182.

45. Riederer, M.S.; Requist, B.D.; Payne, K.A.; Way, J.D.; Krebs, M.D. Injectable and microporous scaffold of densely-packed, growth factor-encapsulating chitosan microgels. *Carbohydr. Polym.* **2016**, *152*, 792–801, doi:10.1016/j.carbpol.2016.07.052.

46. Bhattarai, N.; Ramay, H.R.; Gunn, J.; Matsen, F.A.; Zhang, M. PEG-grafted chitosan as an injectable thermosensitive hydrogel for sustained protein release. *J. Control. Release* **2005**, *103*, 609–624, doi:10.1016/j.jconrel.2004.12.019.

47. Singh, P.; Medronho, B.; Alves, L.; da Silva, G.J.; Miguel, M.G.; Lindman, B. Development of carboxymethyl cellulose-chitosan hybrid micro- and macroparticles for encapsulation of probiotic bacteria. *Carbohydr. Polym.* **2017**, *175*, 87–95, doi:10.1016/j.carbpol.2017.06.119.

48. Singh, P.; Medronho, B.; Alves, L.; da Silva, G.J.; Miguel, M.G.; Lindman, B. Development of carboxymethyl cellulose-chitosan hybrid micro- and macroparticles for encapsulation of probiotic bacteria. *Carbohydr. Polym.* **2017**, *175*, 87–95, doi:10.1016/j.carbpol.2017.06.119.

49. Mi, F.L.; Sung, H.W.; Shyu, S.S.; Su, C.C.; Peng, C.K. Synthesis and characterization of biodegradable TPP/genipin co-crosslinked chitosan gel beads. *Polymer (Guildf).* **2003**, *44*, 6521–6530, doi:10.1016/S0032-3861(03)00620-7.

50. Muzzarelli, R.A.A. Genipin-crosslinked chitosan hydrogels as biomedical and pharmaceutical aids. *Carbohydr. Polym.* **2009**, *77*, 1–9, doi:10.1016/j.carbpol.2009.01.016.

51. Buranachai, T.; Praphairaksit, N.; Muangsin, N. Chitosan/polyethylene glycol beads crosslinked with tripolyphosphate and glutaraldehyde for gastrointestinal drug delivery. *AAPS PharmSciTech* **2010**, *11*, 1128–1137, doi:10.1208/s12249-010-9483-z.

52. Bratskaya, S.; Skatova, A.; Privar, Y.; Boroda, A.; Kantemirova, E.; Maiorova, M.; Pestov, A. Stimuli-responsive dual cross-linked n-carboxyethylchitosan hydrogels with tunable dissolution rate. *Gels* **2021**, *7*, doi:10.3390/gels7040188.

53. Skuredina, A.A.; Tychinina, A.S.; Le-Deygen, I.M.; Golyshev, S.A.; Belogurova, N.G.; Kudryashova, E. V. The formation of quasi-regular polymeric network of cross-linked sulfobutyl ether derivative of β-cyclodextrin synthesized with moxifloxacin as a template. *React. Funct. Polym.* **2021**, *159*, 104811, doi:10.1016/j.reactfunctpolym.2021.104811.

54. Larsson, M.; Huang, W.C.; Hsiao, M.H.; Wang, Y.J.; Nydén, M.; Chiou, S.H.; Liu, D.M. Biomedical applications and colloidal properties of amphiphilically modified chitosan hybrids. *Prog. Polym. Sci.* **2013**, *38*, 1307–1328, doi:10.1016/j.progpolymsci.2013.06.009.

55. Prabaharan, M.; Mano, J.F. Chitosan-based particles as controlled drug delivery systems. *Drug Deliv. J. Deliv. Target. Ther. Agents* **2005**, *12*, 41–57, doi:10.1080/10717540590889781.

56. Larsson, M.; Huang, W.C.; Hsiao, M.H.; Wang, Y.J.; Nydén, M.; Chiou, S.H.; Liu, D.M. Biomedical applications and colloidal properties of amphiphilically modified chitosan hybrids. *Prog. Polym. Sci.* **2013**, *38*, 1307–1328, doi:10.1016/j.progpolymsci.2013.06.009.

57. Vasile, C.; Pamfil, D.; Stoleru, E.; Baican, M. New developments in medical applications of hybrid hydrogels containing natural polymers. *Molecules* **2020**, *25*, 1–68, doi:10.3390/molecules25071539.

58. Charhouf, I.; Bennamara, A.; Abdelmjid, A.; Berrada, M. Characterization of a Dialdehyde Chitosan Generated by Periodate Oxidation International Journal of Sciences : Basic and Applied Research Characterization of a Dialdehyde Chitosan Generated by Periodate Oxidation. **2014**.

59. Samal, S.K.; Dash, M.; Vlierberghe, S. Van; Kaplan, D.L.; Chiellini, E.; Blitterswijk, C. van; Moroni, L.; Dubruel, P. Cationic polymers and their therapeutic potential. *Chem. Soc. Rev.* **2012**, *41*, 7147–7194, doi:10.1039/c2cs35094g.

60. Prabaharan, M. Chitosan-based nanoparticles for tumor-targeted drug delivery. *Int. J. Biol. Macromol.* **2015**, *72*, 1313–1322, doi:10.1016/j.ijbiomac.2014.10.052.

61. Bhattarai, N.; Gunn, J.; Zhang, M. Chitosan-based hydrogels for controlled, localized drug delivery. *Adv. Drug Deliv. Rev.* **2010**, *62*, 83–99, doi:10.1016/j.addr.2009.07.019.

62. Chung, Y.C.; Su, Y.P.; Chen, C.C.; Jia, G.; Wang, H.L.; Wu, J.C.G.; Lin, J.G. Relationship between antibacterial activity of chitosan and surface characteristics of cell wall. *Acta Pharmacol. Sin.* **2004**, *25*, 932–936.

63. Zlotnikov, I.D.; Ezhov, A.A.; Ferberg, A.S.; Krylov, S.S.; Semenova, M.N.; Semenov, V. V; Kudryashova, E. V Polymeric Micelles Formulation of Combretastatin Derivatives with Enhanced Solubility , Cytostatic Activity and Selectivity against Cancer Cells. **2023**.

64. Alvarez-Ordóñez, A.; Mouwen, D.J.M.; López, M.; Prieto, M. Fourier transform infrared spectroscopy as a tool to characterize molecular composition and stress response in foodborne pathogenic bacteria. *J. Microbiol. Methods* **2011**, *84*, 369–378, doi:10.1016/j.mimet.2011.01.009.

65. Razzaghi-Abyaneh, M.; Yoshinari, T.; Shams-Ghahfarokhi, M.; Rezaee, M.B.; Nagasawa, H.; Sakuda, S. Dillapiol and apiol as specific inhibitors of the biosynthesis of aflatoxin G1 in Aspergillus parasiticus. *Biosci. Biotechnol. Biochem.* **2007**, *71*, 2329–2332, doi:10.1271/bbb.70264.

66. Jacobson, T.A. Comparative pharmacokinetic interaction profiles of Pravastatin, Simvastatin, and Atorvastatin when coadministered with cytochrome P450 inhibitors. *Am. J. Cardiol.* **2004**, *94*, 1140–1146, doi:10.1016/j.amjcard.2004.07.080.

67. Tanaka, E. Clinically important pharmacokinetic drug-drug interactions: Role of cytochrome P450 enzymes. *J. Clin. Pharm. Ther.* **1998**, *23*, 403–416, doi:10.1046/j.1365-2710.1998.00086.x.

68.   Zlotnikov, I.D.; Malashkeevich, S.M.; Belogurova, N.G.; Kudryashova, E. V. Thermoreversible Gels Based on Chitosan Copolymers as "Intelligent" Drug Delivery System with Prolonged Action for Intramuscular Injection. *Pharmaceutics* **2023**, *15*, doi:10.3390/pharmaceutics15051478.

69.   Amin, M.; Abbas, N.S.; Hussain, M.A.; Edgar, K.J.; Tahir, M.N.; Tremel, W.; Sher, M. Cellulose ether derivatives: a new platform for prodrug formation of fluoroquinolone antibiotics. *Cellulose* **2015**, *22*, 2011–2022, doi:10.1007/s10570-015-0625-z.

70.   Abbas, N.S.; Amin, M.; Hussain, M.A.; Edgar, K.J.; Tahir, M.N.; Tremel, W. Extended release and enhanced bioavailability of moxifloxacin conjugated with hydrophilic cellulose ethers. *Carbohydr. Polym.* **2016**, *136*, 1297–1306, doi:10.1016/j.carbpol.2015.10.052.

71.   Riederer, M.S.; Requist, B.D.; Payne, K.A.; Way, J.D.; Krebs, M.D. Injectable and microporous scaffold of densely-packed, growth factor-encapsulating chitosan microgels. *Carbohydr. Polym.* **2016**, *152*, 792–801, doi:10.1016/j.carbpol.2016.07.052.

72.   Zlotnikov, I.D.; Streltsov, D.A.; Ezhov, A.A. Smart pH- and Temperature-Sensitive Micelles Based on Chitosan Grafted with Fatty Acids to Increase the Efficiency and Selectivity of Doxorubicin and Its Adjuvant Regarding the Tumor Cells. **2023**.

73.   Zlotnikov, I.D.; Streltsov, D.A.; Belogurova, N.G.; Kudryashova, E. V. Chitosan or Cyclodextrin Grafted with Oleic Acid Self-Assemble into Stabilized Polymeric Micelles with Potential of Drug Carriers. *Life* **2023**, *13*, doi:10.3390/life13020446.